NASA Contractor Report 4548

Effect of Thermal Processing Practices on the Properties of Superplastic Al-Li Alloys

Stephen J. Hales
Analytical Services & Materials, Inc.
Hampton, Virginia

Henry E. Lippard
Northwestern University
Evanston, Illinois

Prepared for
Langley Research Center
under Contract NAS1-19399

National Aeronautics and
Space Administration
Office of Management
Scientific and Technical
Information Program
1993

TABLE OF CONTENTS

LIST OF TABLES

LIST OF FIGURES

EFFECT OF THERMAL PROCESSING PRACTICES ON THE PROPERTIES OF SUPERPLASTIC AL-LI ALLOYS

* Stephen J. Hales[+] and Henry E. Lippard[++]

[+]Analytical Services & Materials, Inc.
107 Research Drive
Hampton, VA 23666

[++]Department of Materials Science
Northwestern University
2225 Sheridan Road
Evanston, IL 60208

ABSTRACT

The effect of thermal processing on the mechanical properties of superplastically formed structural components fabricated from three aluminum-lithium alloys was evaluated. The starting materials consisted of 8090, 2090 and X2095 (Weldalite™ 049), in the form of commercial-grade superplastic sheet. The experimental test matrix was designed to assess the impact on mechanical properties of eliminating solution heat treatment and/or cold water quenching from post-forming thermal processing. The extensive hardness and tensile property data compiled are presented as a function of aging temperature, superplastic strain and temper/quench rate for each alloy. The tensile properties of the materials following superplastic forming in two T5-type tempers are compared with the baseline T6 temper. The implications for simplifying thermal processing without degradation in properties are discussed on the basis of the results.

* Dr. S.J. HALES, Research Scientist, was working in support of the National Launch System Program in the Materials Division at NASA Langley Research Center. Mr. H.E. LIPPARD, currently a graduate student, was in the Materials Division as a Langley Aerospace Research Summer Scholar during 1990-92.

1. INTRODUCTION

The integration of superplastic forming (SPF) of aluminum-lithium (Al-Li) alloys with built-up structure concepts is being evaluated for the fabrication of lightweight launch vehicles [1,2]. The application of SPF technology has the potential to improve the structural efficiency of both the cryogenic tank and dry bay assemblies. The exceptional formability permits the manufacture of complex-shapes and the reproducibility allows for close tolerances [3]. The benefit of Al-Li alloys centers around the improved specific properties compared to conventional Al alloys. The candidate materials in this activity are the commercial superplastic versions of 8090, 2090 and X2095 (formerly Weldalite™ 049), which offer advantages for both strength- and stiffness-critical applications. By using Al-Li built-up structures, the structural weight savings on future launch systems are expected to be appreciable.

The performance of superplastically formed material will be governed by both the ***SPF parameters*** employed and the ***post-SPF thermal processing*** selected. Although not addressed in detail in this study, the forming parameters are chosen on the basis of ensuring complete part formation without localized thinning and, simultaneously, suppressing cavitation. Standard post-forming practices for Al alloy SPF components include heat treatment to place the material in a close to peak strength condition. This slightly underaged T6 temper is preferable because cold stretching of complex-shaped components for a T8-type temper tends to be impractical [4]. As outlined in Figure 1, post-SPF processing traditionally involves uncontrolled air cooling from forming temperatures of 900-1000°F (480-540°C), solution heat treatment (SHT) at temperatures the same as, or higher than, the SPF temperature (T_{SPF}), followed by cold water quenching (CWQ). After correcting for any distortion due to the rapid cooling, a low-temperature aging treatment is subsequently used to attain the T6 temper condition [4].

Streamlining of the post-SPF thermal processing procedures outlined is desirable from the perspective of cost-effective manufacturing. First, application of SPF technology will be most economical when the number of processing operations is minimized. More complicated shapes can be produced compared to conventional fabrication practices, but forming cycles are relatively long [3]. Second, less severe quenching will reduce the amount of costly re-work required to retain dimensional conformance. Distortion caused by rapid cooling from elevated temperatures tends to be amplified in thin-gage components and geometric reproducibility will be a prerequisite for structural applications [3,6]. Third, decreasing the duration of exposure to temperatures above 900°F (480°C) in air during thermal processing will minimize solute depletion effects [7-9]. The presence of solute-lean surface regions can be detrimental to the performance of Al-Li sheet materials [7].

The objective of this research was to assess the potential to simplify post-SPF thermal processing through elimination of the SHT and/or CWQ stages characteristic of T6 processing [5]. As illustrated in Figure 1, removal of SHT will result in a T5-type temper following artificial aging. The T5 condition, which is a user-specified temper, is broadly defined as; "material which has been cooled from an elevated-temperature shaping process and artificially aged" [4]. The economic advantages mentioned will only be realized providing that it can be

demonstrated that replacing T6 with T5 thermal processing does not result in significant degradation of mechanical properties [6]. The systematic approach adopted here for evaluating the 8090, 2090 and X2095 alloy components was designed to permit a direct comparison of the post-SPF tensile properties of bulk material as a function of temper selection.

2. EXPERIMENTAL APPROACH

2.1 VINTAGE OF THE SPF MATERIAL

The compositions of the commercial superplastic Al-Li alloys employed in this investigation, in comparison to the specified ranges, are presented in Table I. The 2.3 mm thick sheet product of the three alloys was designated 8090-SP, 2090-OE16 and X2095-RT72 produced by British Alcan, ALCOA and Reynolds Metals, respectively. The 8090 and 2090 materials were commercial-grade superplastic versions of the alloys received in the form of 2.5 x 1.25 m and 3.75 x 1.25 m sheets, respectively. X2095 is registered with the Aluminum Association as the experimental alloy designation for Weldalite™049 variants containing 3.9-4.6 wt.pct. Cu. The target Cu content for the batch of material (#63522) used in this study was the upper limit of the range specified for X2095. Although the 1.0 x 0.5 m superplastic sheets received were produced on a pilot plant scale from 180 kg ingots, the material was processed using the thermomechanical treatment established for commercial-scale product. Therefore, the material was considered near-commercial grade for the purposes of the investigation.

Table I. Superplastic Al-Li Alloy Compositions (Wt.Pct.)

ALLOY		Cu	Li	Mg	Ag	Zr	Fe	Si
8090	Range	1.0 - 1.6	2.2 - 2.7	0.6 - 1.3	---	0.04 - 0.16	0.30 max	0.20 max
	Meas.	1.32	2.41	0.60	---	0.11	0.05	0.09
2090	Range	2.4 - 3.0	1.9 - 2.6	0.25	---	0.08 - 0.15	0.12 max	0.10 max
	Meas.	2.55	2.16	0.01	---	0.11	0.07	0.06
X2095	Range	3.9 - 4.6	1.0 - 1.6	0.25 - 0.6	0.25 - 0.6	0.04 - 0.18	0.15 max	0.12 max
	Meas.	4.64	1.22	0.39	0.39	0.13	0.07	0.05

Comparison of existing post-SPF property data from different sources tends to be complicated by a lack of documentation regarding the as-formed condition of the material. An

example of one of the 0.3 x 0.2 m superplastically formed 'pans' from which material was extracted to perform thermal processing studies is shown in Figure 2. The forming parameters used, which were optimized for apparatus with 500 psi maximum gas pressure capability, are presented in Table II [2]. The temperature, strain rate and corresponding flow stress (σ_f) had been established previously for the specific materials from extensive uniaxial and biaxial testing. Details concerning derivation of the pressure-time profiles used for fabricating these structural components at a constant biaxial forming rate have been described elsewhere [10, 11]. It was considered critical to the success of this study that the mechanical property data were not compromised by the presence of voids in the as-formed materials [6]. Cavitation was effectively suppressed by superimposed back pressure ($0.5\text{-}0.7\sigma_f$) during SPF and a post-forming pressure cycle involving a specified dwell time at 500 psi [1].

Table II. Superplastic Forming Parameters Employed

ALLOY	Temperature		Strain Rate	Flow Stress		Back Pressure	
	°F	°C	$x10^{-4}s^{-1}$	ksi	MPa	psi	MPa
8090	985	530	2.5	0.45	3.1	325	2.2
2090	950	510	5.0	0.60	4.1	350	2.4
X2095	925	496	6.0	0.80	5.5	400	2.8

Figure 2 also identifies the various elements of the SPF structural component in conjunction with the predominant level of SPF true thickness strain associated with each area. Examples of the locations and orientation of tensile blanks extracted from the component are also indicated. Definition and determination of SPF strain have been presented previously [11] and the thickness, equivalent engineering strain and true thickness strain as a function of location are listed in Table III for reference. The ranges shown reflect the thickness tapering which is inherent to SPF components and the weighted averages indicate the predominant level of SPF strain within the different regions of a typical pan. The table shows that material extracted from the frame and sides of the SPF pan provided hardness coupons with the same overall range of SPF strain as the actual component.

2.2 EXPERIMENTAL PROCEDURES

2.2.1 Design of the Experiment

A reproducible starting condition for all three materials was considered essential to the design of an effective artificial aging experiment. First, microhardness testing was used to determine the extent of solute depletion. It was deemed necessary to remove any soft surface layers such that the macrohardness and tensile data acquired were truly representative of bulk material. In the absence of direct measurement of Li concentrations, microhardness testing was considered the most appropriate technique [12]. Microhardness profiles as a function of depth

were determined for the three materials in an approximate T6 temper. It was anticipated that the ≈ 3 hrs exposure to temperatures in excess of 900°F (480°C), resulting from both SPF and SHT, would represent the worse case scenario with respect to solute depletion [7].

Table III. SPF Strain as a Function of Location in Formed Parts

Location:		Frame	Side	Cap	Web	Flange
Thickness (mm)		2.3	1.8 - 1.1	1.9 - 1.7	1.7 - 0.7	1.5 - 0.7
Equiv. Strain (%)	Range	0	30 - 100	20 - 40	40 - 220	50 - 220
	Average	0	65	35	65	80
True Strain	Range	0	0.3 - 0.7	0.2 - 0.3	0.3 - 1.2	0.4 - 1.2
	Average	0	0.5	0.3	0.5	0.6

Second, macrohardness testing was used to determine the natural aging behavior of the materials following cooling from the SPF die. It was considered imperative that the initial material was in a stable condition, such that any effect due to varying amounts of natural aging was avoided. The T1 temper was selected, which is defined as; "material which has been cooled from an elevated shaping process and naturally aged to a substantially stable condition" [4]. Natural aging studies were conducted on freshly formed components, cooled by CWQ or AAC, and sectioned to permit hardness evaluation of the material mid-plane. The time at room temperature required to achieve a stable hardness governed the lead time between SPF and post-SPF heat treatment activities. In the baseline T6 thermal processing schedule the materials were allowed a minimum of 72 hrs at room temperature between SHT and artificial aging. This interval was chosen to duplicate the common practice in industry [5].

An extensive review of current literature concerning post-SPF property data was used as the basis for designing a manageable experiment [e.g. 13-18]. The matrix was formulated to establish optimum aging treatments for maximum strength with adequate ductility (5% min.) using practical aging times (8-40 hrs). The variables included in the experiment for all three alloys are outlined in Table IV. The three levels of SPF strain selected were dictated by the geometry of the biaxially-formed SPF components and the limited amount of flat material available for extracting tensile blanks. Two modifications to the baseline T6 temper were considered; (a), eliminating the SHT to produce a T5/CWQ temper, and (b), eliminating the SHT stage and replacing the CWQ with accelerated air cooling (AAC), to produce a T5/AAC temper. It should be noted that the T6/AAC permutation was not included in the investigation.

The term 'accelerated' air cooling refers to the use of a fan to create air movement over the hot component, which is distinct from 'still' air cooling (SAC), involving stationary air, or 'forced' air cooling (FAC), involving directed (compressed) air flow. AAC produces a cooling rate intermediate between the two latter categories, such that the quench media selected bracket

the cooling rates following either SPF or SHT in common practice. In selecting the range of aging treatments, the intent was to limit the experimental matrix to a realistic number of temperature/time combinations. Temperatures of 325, 350 and 375°F (163, 177 and 191°C) were selected and times ranging from 1 to 100 hrs were chosen for identifying a peak-aging treatment of practical duration.

Table IV. Summary of Variables Included in Experimental Matrix

Al-Li Alloy	SPF Strain		Temper	Quench Rate	Aging Treatment		
	Equiv.	True			Temperature		Time
	%				°F	°C	Hrs
8090	0	0	T6	CWQ	325	163	1 3 10
2090	35	0.3	T5	AAC	350	177	16 24 40
X2095	80	0.6			375	191	60 100

2.2.2 Evaluation of Mico- and Macro-Hardness

The material used for microhardness evaluation was extracted from the mid-point of the web section of a formed pan (Fig. 2), which corresponded to the median strain of 0.5 for the SPF components (Table III). Placing the materials in the vicinity of peak hardness, as determined from existing literature [e.g. 13-18], allowed the trends in microhardness to be readily discerned. Microhardness testing was conducted using the Knoop scale (with 2g load) following standard metallographic surface preparation techniques. Testing procedures conformed with ASTM E384 specifications for through-thickness measurements [19]. Data were compiled at 25 μm intervals in the through-thickness direction from both surfaces and each datapoint represented an average of ≥ 10 tests. Profiles of microhardness as a function of depth were constructed to determine the amount of surface material needed to be removed prior to mechanical testing. The surface layers were removed using a standard caustic etch/de-smut technique owing to the large number of coupons required for macrohardness evaluation. It was established that the final gage of the thinnest coupons (0.6 SPF strain material) was above the minimum thickness specified for the acquisition of valid data on the hardness scales employed [20].

The relative ease of macrohardness data collection allowed the full matrix of variables listed in Table IV to be assessed. One of the initial concerns was the choice of an appropriate hardness test. The Rockwell superficial hardness scales were selected for the acquisition of valid data from the thin-gage material that is inherent to SPF parts. Hardness testing was performed

in accordance with ASTM E18 specifications [20]. As a consequence of the reduced penetration depths associated with superficial-type tests, there tends to be an increase in variability compared to more conventional hardness tests. Therefore, each datapoint represented the mean of a minimum of 9 hardness tests. The number of repetitions was increased to improve statistical accuracy in instances where the data scatter was considered unacceptable. A high level of confidence in the hardness data was a prerequisite to the design of a reduced tensile test matrix capable of identifying the trends in strengthening behavior.

2.2.3 Evaluation of Tensile Properties

The sequence for specimen preparation was considered very important from the perspective of the thickness tapering inherent to post-SPF material, the potential for solute depleted zones in Al-Li alloys and quench distortion in sheet-gage materials. It was necessary to eliminate any detrimental effect on tensile properties associated with varying thickness, soft surface layers or warped specimens for the results to be representative of bulk properties. For tensile specimen preparation, the post-SPF materials were in the T1 condition for heat treatment to the T5-type tempers, and the T4 condition for aging to the T6 temper. In the latter instance, material was solution treated prior to any machining to circumvent exposure of the finished tensile specimens to temperatures above 900°F (480°C). Specimen distortion as result of rapid cooling was averted by conducting CWQ operations prior to sectioning of the self-reinforcing SPF pans. Quench distortion will be more problematic for full-scale components in which the formed area will be much larger than the undeformed perimeter.

The machining sequence adopted involved extracting the blanks and grinding each blank to a uniform gage. The final thickness was such that any solute depleted layers in the areas corresponding to the gage sections were removed. Subsequent operations involved final machining of the flat blanks to dimensions which conformed with ASTM B557 specifications [21]. The tensile specimens were then exposed to low-temperature artificial aging treatments to place the materials in the various conditions specified by the test matrix. The tensile testing was performed under cross-head displacement control with a strain rate at yield of $\approx 10^{-4}$ s^{-1} as the target. The load at yield was determined from the standard 0.2% offset method and the stresses were calculated using three thickness and width measurements taken along the length of the reduced section prior to testing. Elastic modulus was estimated from the slope of the stress-strain curves and elongations were measured with back-to-back, 25 mm gage extensometers.

The limited availability of standard sub-size rectangular test specimens from the SPF pans dictated that only a partial tensile test matrix could be performed with adequate repetitions. The extensive macrohardness data compiled was used as a screen to select appropriate aging times for establishing the overall strengthening response from a much smaller test matrix. Results from the hardness testing also indicated a negligible effect of SPF strain on properties in the range of 0 to 0.6. Therefore, the tensile data were compiled primarily for 0.6 strain material and the 0 and 0.3 strain specimens (Fig.2) were retained for any follow-up tests required to clarify inconsistencies in the initial data.

3. RESULTS AND DISCUSSION

3.1 INITIAL MATERIAL CONDITION

3.1.1 Surface Solute Depletion

Microhardness testing allowed the extent of the solute depleted layers in the three alloys to be assessed. The depth profiles shown in Figure 3 reveal that solute loss has a considerable effect on surface hardness as a result of T6 processing. The softened surface layer is $\approx$ 200 μm in both 8090 and 2090 and $\approx$ 150 μm in X2095. It is apparent that the depth of the depleted layer increases in proportion to the Li content of the particular alloy, as shown in Table I. The depths represent $\approx$ 30 percent of the cross-sectional area of the 0.6 strain material used for most of the tensile property evaluation ($\approx$ 1.3 mm thick). Solute depletion can be reduced by conducting the SHT step in an inert atmosphere, but performing the subsequent CWQ step on multiple components becomes problematic. Therefore, in order to eliminate solute depletion effects, it was necessary to remove a minimum of 200 μm of material from both sides of the materials prior to testing. As outlined earlier, this was subsequently achieved by chemical milling of the hardness coupons and mechanical grinding of the tensile specimens.

The effect of solute depletion on tensile properties would be expected to be greatest in the peak-aged condition when the differential between surface and bulk properties will be at a maximum. For this reason, it will be necessary to account for any effect of solute depletion in engineering applications of Al-Li alloys. However, recent attempts to correlate degradation in properties with Li-depletion have encountered difficulties [22]. Thermal processing using inert (pressurized) atmospheres and salt baths, in addition to coatings and Al-cladding, are currently being evaluated [e.g. 14,23]. The primary aim of determining the extent of Li depletion was to determine the quantity of surface material to be removed to provide for a direct comparison between the bulk properties of superplastic Al-Li alloys. The benefits of developing a standard practice for specimen preparation were that the influence of thermal processing on tensile properties could be assessed. The experimental approach permitted the effect of processing variables on aging response to be isolated for the individual alloys and also allowed a comparison between alloys.

3.1.2 Natural Aging Response

The aim of the natural aging studies was to identify the dwell time required to achieve a T1 temper condition in each of the alloys following SPF. Data collection was extended to over 8000 hrs at ambient temperature in order to fully characterize the natural aging response. The results presented in Figure 4 are by way of illustration for 0.6 strain material following both CWQ and AAC from the SPF die. It is clear that 8090 exhibits the strongest natural aging response with an increase in hardness from 21 to 57 HR30T over the aging times evaluated. The hardening response is sigmoidal in behavior using either CWQ or AAC from T_{SPF}. For CWQ material, the rate of hardening increases after $\approx$ 10 hrs, maintains a constant high rate and then gradually decreases after $\approx$ 100 hrs. Maximum hardness is achieved following $\approx$ 500 hrs natural aging with no change thereafter. For the AAC material, the final hardness attained

is the same, the response only differing in that the delay preceding rapid hardening is extended to ≈ 24 hrs and a plateau in hardness is reached following ≈ 1000 hrs of natural aging.

The curves for X2095 also show a strong natural aging response; CWQ material increasing from 42 to 70, and AAC material from 44 to 67 HR30T. The behavior differs from that observed for 8090 in that the rate of hardening gradually decreases as natural aging time increases. The maximum hardness achieved following AAC is marginally lower than that achieved following CWQ. Of improtance is the fact that in both cases the rate of hardening becomes negligible after ≈ 1000 hrs at ambient temperature. In contrast, 2090 exhibits a much weaker natural aging response, with the hardness only increasing from 30 to 42 HR30T for CWQ material, and to 37 HR30T for AAC material in 8000 hrs. The curves are similar to the initial 8090 behavior in that the onset of hardening is delayed. The rate of hardening gradually increases with aging time after ≈ 100 hrs following either quench rate from T_{SPF}. The differential in final hardness level is similar to the X2095 case, although a plateau in hardness is not evident after extensive natural aging of 2090.

Rationalization of the data reveals that the extent of natural aging appears to be inversely related to the differential between the SHT temperature (T_{SHT}) and T_{SPF}, as noted in Table V. For example, the increase in hardness for material following CWQ from T_{SPF} are 12, 28 and 36 for 2090, X2095 and 8090, respectively. Therefore, the differences in natural aging behavior probably reflect the degree of solute saturation, with only post-SPF 8090 material being in a fully solution treated condition. In contrast, X2095 and 2090 exhibit a decreased hardening response as a consequence of being in a partially solution treated condition at the conclusion of forming. It is noteworthy that there does not seem to be a correlation between the natural aging behavior and the Cu, Li or total solute content of the alloys (8090; 4.3 wt%, 2090; 4.7 wt% and X2095; 6.0 wt%).

Table V. Difference between SPF and SHT Temperatures

Alloy	T_{SPF}		T_{SHT}		*Difference*	
	°F	°C	°F	°C	*°F*	*°C*
8090	985	530	985	530	*0*	*0*
2090	950	510	1000	538	*50*	*28*
X2095	925	496	940	504	*15*	*8*

The natural aging behavior documented indicates that the 72 hr lead time commonly used in industry for a material to be considered in a T1 temper is inappropriate. The materials were not in a "substantially stable" condition until 1000 hrs at ambient temperature on the basis of the 8090 and X2095 data and the relatively weak response observed for 2090. Therefore, following SPF material was held for 1000 hrs prior to both solution treatment and aging for T6 processing, and before aging only for T5 processing. Although this does not represent a practical lead time,

data comparability was considered an important issue during inception of the experiment. It is not implied that this amount of natural aging is necessary or will be required in the application of these alloys.

3.2 AGE HARDENING BEHAVIOR

As a consequence of the broad scope of the experimental matrix, only results which best reveal the trends are presented in the text. All of the data compiled are presented in the appendix for reference. The influence of thermal processing on post-SPF properties is addressed by dividing the effects of the experimental variables listed in Table IV into three distinct categories. Consequently, the data are presented as a function of ***Aging Temperature***, ***SPF Strain*** and ***Temper/Quench Rate***. Assessment of the first category allowed the most appropriate aging temperature to be selected. Subsequently, data concerning the effect of SPF strain and temper/quench rate on aging response at that temperature only are presented. The hardness data was conducted using the HR30T scale for 8090 and 2090 material. The HR45T scale was used for X2095 material, since preliminary measurements revealed that the hardnesses were above the specified range for the HR30T scale.

3.2.1 As a Function of Aging Temperature

Figure 5 demonstrates the difference in age hardening behavior of superplastically formed 8090, 2090 and X2095 as a function of aging temperature. Material had been deformed to 0.6 strain, CWQ from T_{SPF} and naturally aged for 1000 hrs. The data presented are for artificial aging at 325, 350 and 375°F (163, 177 and 191°C), each datapoint representing the average of at least 9 hardness measurements. The figure shows that the location of the peak moves to shorter times and the height of the peak decreases with increasing aging temperature. This general trend is consistent with the common observation in superplastic Al-Li alloys that the maximum attainable hardness increases with decreasing aging temperature in the range of 250-375°F (120-190°C) [e.g. 13-18]. In addition, natural aging followed by low-temperature underaging tends to produce desirable strength-toughness combinations in these alloys [24]. Therefore, the lowest aging temperature, while maintaining a practical aging time (i.e. $\leq$40 hrs), will potentially yield the best tensile properties.

In Figure 5(a), the curves reveal that the peak aging times for 8090 are $>$100, 60 and 24 hrs for aging at 325, 350 and 375°F, respectively. Upon consideration of a practical peak aging time, 375°F would appear to be the aging temperature of choice. However, Al-Li alloys are usually used in a slightly underaged condition which produces a desirable balance of mechanical properties. From this perspective, selecting 350°F as the aging temperature will provide greater flexibility in specifying an underaging time of 8-40 hrs. It is noteworthy in Figure 5(a) that the level of hardness following underaging at 350°F for 40 hrs is the same as the peak hardness for aging at 375°F. The data in Figure 5(b) reveal that 2090 behaves in a very similar manner to 8090. The peak aging time is $>$100 hrs at 325°F, 50 hrs at 350°F and 30 hrs at 375°F, accompanied by a small decrease in peak height. An aging temperature of 350°F appears to be the best candidate for defining a practical underaging heat treatment time.

Again, the hardness following aging for ≈ 30 hrs at 350°F is the same as the peak hardness for aging at 375°F.

In Figure 5(c), the peak hardness is achieved at > 100, 40 and 16 hrs for aging of X2095 at the three respective temperatures. Upon consideration of the hardness scale and range employed on the ordinate axis, the hardness increase is large during artificial aging of this alloy. It is clear that 350°F is the temperature which produced a peak within the range of practical aging times. The difference in the aging behavior at the three temperatures is more pronounced with X2095 than with 8090 and 2090. The hardness of the material following 1 hr of artificial aging is markedly below the T1 hardness of the material for all three temperatures. This is in contrast to the behavior of 8090 and 2090 in which the hardness after 1 hr of artificial aging was close to the level observed at the conclusion of natural aging. A strong aging response at room temperature and a reversion in hardness following short-time artificial aging of fully naturally aged material have been noted previously for Weldalite™ alloys [26-28]. The X2095 data presented are consistent with other post-SPF data which suggest that the extent to which the hardness is depressed during the reversion is a function of aging temperature [18].

3.2.2 As a Function of SPF Strain

Figure 6 shows the age hardening behavior of 8090, 2090 and X2095 as a function of SPF strain for material starting in a T1 condition following CWQ from T_{SPF}. The data presented are for material which has been superplastically formed to strains of 0, 0.3 and 0.6 followed by artificial aging at 350°F. The 8090 data in Figure 6(a) show that the peak location and height is unaffected by superplastic deformation in the range of 0-0.6 SPF true strain. The curves pertaining to the 0 and 0.3 strain material are the same within experimental limits [20], but the hardness following 1 hr aging at 350°F for 0.6 strain material is lower. This results in a marginal increase in the rate of hardening up to the peak, but no change in peak height or location.

The 2090 data shown in Figure 6(b) bear a close resemblance to the 8090 data. The difference between the peak hardnesses of 2 points can be considered negligible based on the quoted accuracy of ±1 point for the HR30T scale [20]. The behavior of the 0 and 0.3 material is the same over the range of aging times, but the hardness after 1 hr aging is lower for the 0.6 material. Again, the rate of hardening is higher for the latter material, such that the peak location is unaffected by the initial difference. The data for X2095 presented in Figure 6(c) reveal the same trend. It is important to note the different hardness scale and range on the ordinate axis of this plot. The curves show that the variation in SPF strain between 0 and 0.3 has a negligible effect, but the 0.6 strain material has an initial hardness 5 points lower. Again, the peak hardness and peak aging time is not affected by differences in strain. The rate of hardening between 1 and 10 hrs is much higher than for 8090 and 2090 regardless of strain level as a result of the reversion phenomenon alluded to earlier [18].

3.2.3 As a Function of Temper/Quench Rate

The aging behavior of 8090, 2090 and X2095 at 350°F for the T6, T5/CWQ and T5/AAC tempers is presented in Figure 7. In all cases the material had been deformed to 0.6

strain and naturally aged to a T1 condition (1000 hrs) following SPF for T5 processing and a T4 condition (72 hrs) following SHT for T6 processing. The effect of eliminating SHT can be evaluated by comparising the aging behavior for a T5-type temper with that for a T6 temper. Of equal concern is the influence on the T5 hardening response of replacing CWQ with AAC on removal of SPF components from the die. It is important to consider the temperature difference between T_{SHT} and T_{SPF} when evaluating the relative quench sensitivity of the alloys during T5 processing. Therefore, the temperature differential associated with each alloy is presented in Table V for reference.

The post-SPF age hardening response of 8090 as a function of temper/quench rate is illustrated in Figure 7(a). The curves show that the aging behavior is relatively unaffected by the starting condition of the material, with respect to peak location. The peak aging time is 60 hrs, regardless of which temper is selected. The peak heights for all three tempers are very similar, but the peak hardness for the T5/AAC temper is slightly higher. It is also interesting to note that the T6 peak hardness appears to be intermediate between the T5/AAC and the T5/CWQ hardness levels. The lack of appreciable differences can be attributed to forming at T_{SHT} and to the lack of quench sensitivity documented for this alloy [31]. This has been cited as major benefit associated with the processing of 8090-SP material [32].

In Figure 7(b), the aging response of 2090 as a function of temper/quench rate is presented. The data reveal the degradation in properties typically associated with eliminating SHT and employing slower cooling rates for a quench sensitive alloy [30]. The drop in peak hardness from T6 to T5/CWQ reflects the large differential between the SHT and T_{SPF}. As noted in Table V, the temperature difference of 50°F is significant compared to the other two alloys. The peak aging time of 60 hrs is the same for the two tempers, even though material for the T5/CWQ temper was initially in a partially solution treated condition. The drop in peak hardness from T5/CWQ to T5/AAC reflects the quench sensitivity of the alloy from T_{SPF}. It has been shown that slower cooling of 2090 results in fewer, coarser strengthening precipitates during subsequent artificial aging [33,34]. This explains the lower peak hardness for the T5/AAC condition and may also account for the reduction in the peak aging time to 24-40 hrs.

The data pertaining to the effect of temper/quench rate on the aging response of X2095 are presented in Figure 7(c). Again, attention should be drawn to the different hardness scale and range employed to construct the plot. Comparing the curves for the T5/CWQ temper with the T6 temper reveals that eliminating SHT has a negligible effect on aging behavior. The lack of appreciable differences between peak aging time and hardness for the two tempers could be related to the small (15°F) temperature differential between T_{SHT} and T_{SPF}. In contrast, replacing CWQ with AAC in the T5 temper leads to a considerable reduction in the maximum attainable hardness for X2095. The peak location is still at 40 hrs aging time, but the peak hardness has decreased considerably from the T5/CWQ to the T5/AAC temper condition. This implies that the alloy is quench sensitive during cooling from T_{SPF}, which is consistent with other X2095 post-SPF data for a different T_{SPF}, but with the same nominal Cu content [17]. The degree of quench sensitivity has been linked with Cu content in both 8090 [9] and 2090 [33] and X2095 contains approximately twice the Cu concentration of these alloys.

3.3 STRENGTHENING BEHAVIOR

As a consequence of the volume of data generated, the tensile results which best illustrate the trends in the data are presented. A compilation of all of the tensile data is presented in the appendix for reference. The influence of thermal processing on the post-SPF strengthening behavior of ***8090***, ***2090*** and ***X2095*** is shown in Figures 8, 9 and 10, respectively. The data pertain to material deformed to 0.6 SPF true strain material, naturally aged to a stable condition and artificial aging at a temperature of 350°F. The effects of replacing T6 with T5 processing and replacing CWQ with AAC for a T5-type temper are addressed for each alloy sequentially. Ultimate tensile strength (σ_u), 0.2% offset yield strength (σ_y) and elongation (El.) data are presented as a function of aging time. Each datapoint represents the average of three tensile tests and includes range bars. The ductility data may have been compromised by the tendency of the tensile specimens to break within the reduced section, but outside the specified gage length. Consequently, although determination of strength was unaffected, the values for total elongation provided by the extensometers may be considered conservative.

The impact of processing modifications on peak aged properties is addressed initially followed by assessment of underaged properties. Al-Li alloys are usually used in the slightly underaged condition as a consequence of the materials exhibiting more balanced properties [24,35]. The primary goals of this investigation were to define processing practices readily adaptable to industry and to establish material conditions appropriate to structural application. The recommended aging practice and typical tensile properties for post-SPF 8090, 2090 and X2095 materials are summarized in Table VI for the, (a), peak aged and, (b), slightly underaged condition. Selection of a suitable underaging treatment was based on three criteria;

(i) an aging time of practical duration for commercial application (8-40 hrs)
(ii) adequate ductility for an engineering material (El. $\geq$ 5 %)
(iii) minimal decrease in yield strength compared to the peak value.

3.3.1 Alloy 8090-SP

Figure 8 shows the effect of temper/quench rate selection on the post-SPF tensile properties of 8090. The data associated with achieving the baseline T6 temper, presented in Figure 8(a), show that strength reaches a maximum and ductility a minimum following 40 hrs aging at 350°F. The peak-aged properties consist of σ_u= 73 ksi, σ_y= 59 ksi and El.= 4 %. In Figure 8(b), for the T5/CWQ temper, the peak is located at 60 hrs with σ_u= 73 ksi, σ_y= 59 ksi and El.= 6 %. Thus, there is no change in peak strengths and a 50 percent improvement in ductility associated with T5 processing including rapid cooling. Similarly, for the T5/AAC temper in Figure 8(c), the peak aging time agian is 60 hrs, but there has been a drop in strength as a result of the slower cooling rate from T_{SPF}. The tensile properties following peak aging consist of σ_u= 70 ksi, σ_y= 56 ksi and El.= 6 %. In comparison to the T6 temper, there has been a 4 percent decrease in ultimate strength, a 5 percent decrease in yield strength accompanied by an increase in ductility. A value for the elastic modulus of 8090 was estimated to be 11.8 $\pm$ 0.25 Msi ($\approx$ 81.4 GPa). This value represents an average of the data compiled for material in an approximately peak-aged condition for all three tempers (19 tests total).

Table VI. Typical Post-SPF Tensile Properties of Al-Li Alloys

ALLOY	Temper	Temp/Time °F / Hrs	σ_u ksi	σ_y ksi	$\Delta\sigma_y$* %	El. %
(a) Peak Aged Condition for Maximum Strength						
8090	T6	350 / 40	73	59	--	4
	T5/CWQ	350 / 60	73	59	*0*	6
	T5/AAC	350 / 60	70	56	*-5*	6
2090	T6	350 / 60	72	66	--	3
	T5/CWQ	350 / 24 +	69	56	*-15*	6
	T5/AAC	350 / 24 +	70	57	*-15*	6
X2095	T6	350 / 16	94	90	--	4
	T5/CWQ	350 / 24	97	95	*+5*	3
	T5/AAC	350 / 24	82	71	*-20*	4
(b) Underaged Condition for Balanced Properties **						
8090	T6	350 / 24	70	57	--	5
	T5/CWQ	350 / 40	70	56	*0*	6
	T5/AAC	350 / 40	69	55	*0*	6
2090	T6	350 / 40	72	62	--	5
	T5/CWQ	350 / 16	66	53	*-15*	6
	T5/AAC	350 / 16	69	55	*-10*	6
X2095	T6	350 / 10 [350/3] ++	92 [77]	87 [60]	--	4 [15]
	T5/CWQ	350 / 10 [350/3] ++	91 [79]	86 [62]	*≈ 0*	4 [14]
	T5/AAC	350 / 16	83	71	*≈ -20*	5

* Change in σ_y resulting from replacing T6 with T5-type processing.

** Selection Criteria : Aging time ≤ 40 hrs; Ductility ≥ 5%; Minimum decrease in σ_y.

\+ Meet criteria; underaged for other properties.

++ 350°F / 8 hrs ; $\sigma_u \approx$ 90 ksi ; $\sigma_y \approx$ 80 ksi ; El. ≈ 5 % (Interpolated from Figure 10).

The full effect of temper selection on 8090 post-SPF properties can be discerned by comparing the hardening data in Figure 7(a) with the strengthening behavior in Figure 8. First, the data are consistent with regards to an aging time of 60 hrs for peak hardness and peak strength regardless of temper. Second, the trends in hardness and strength with increasing aging time are in agreement for each temper. Both ultimate and yield strength follow the hardness data within the limits of experimental accuracy and this correlation has been observed previously during aging of Al-Li alloys [38]. Third, comparing Fig. 7(a) with Fig. 8(b) shows that the lowest hardness and strength values were observed at times of <24 hrs while aging to the T5/CWQ temper. The higher properties for the T5/AAC condition can be explained in terms of the decreased cooling rate and nucleation effects. The discrepancy between the T6 and T5/CWQ data for these aging times is also probably related to microstructural differences.

Examination of the strengthening behavior for the three tempers, Figure 8, reveals that underaging of 8090 results in little improvement in ductility. Aging for 24 hrs at 350°F seems to be appropriate from the perspective of more balanced properties during T6 processing. The peak-aged ductility following T5 processing is already adequate, but the aging time may be considered too long. Reducing the duration to 40 hrs at 350°F does not result in a decrease in strength and the underaged properties for the T5/CWQ and T5/AAC conditions compare favorably with the T6 baseline.

The insignificant changes resulting from eliminating the SHT and CWQ steps from processing can be attributed to T_{SPF} being the same as T_{SHT} and a lack of quench sensitivity. The results imply that the alloy is in a fully solution-treated condition at the conclusion of forming and does not require rapid cooling to retain properties. The typical tensile properties and insensitivity to quench rate documented compare very favorably with the available data on commercial material [9,36]. The net result of these factors is that a T5-type temper can be utilized in place of the T6 temper without significant degradation in tensile properties.

The loss in strength is relatively small if a ≤ 5 percent reduction is selected as the maximum allowable degradation in properties resulting from processing modifications. The data reveal that yield strength is affected more than ultimate strength by using a T5-type temper. Consistent with other studies, it is suggested that this is connected with the increase in ductility observed [37]. The results indicate that replacing CWQ with AAC in T5 processing causes a decrease in yield strength which is beyond the prescribed margin. It is surmised that a cooling rate intermediate between CWQ and AAC from T_{SPF}, such as FAC, will maintain the yield strength within 5 percent of the value for the T6 temper.

3.3.2 Alloy 2090-QE16

The effect of thermal processing on post-SPF 2090 tensile properties is outlined in Figure 9. Data for the baseline T6 temper are presented in Figure 9(a) and the strengthening behavior is similar to the 8090 data. Peak strength is achieved following 60 hrs aging at 350°F and the post-SPF T6 properties consist of $\sigma_u = 72$ ksi, $\sigma_y = 66$ ksi and El. = 3 %. The ductility decreases with increasing aging time to a minimum at the peak-aged condition. In Figure 9(b) for the T5/CWQ temper, the peak is located at 24 hrs, with $\sigma_u = 69$ ksi, $\sigma_y = 56$ ksi and El. =

6 %. The drop in strength compared to the baseline condition is 15 percent for the yield strength and 4 percent for the ultimate strength. The more pronounced decrease in yield strength is accompanied by an increase in ductility. The data for the T5/AAC temper in Figure 9(c) reveal that the peak aging time has been unaffected by the slower quench rate. There has also been no change in the peak-aged properties compared to the T5/CWQ condition. Following 24 hrs of aging, the properties consist of σ_u = 70 ksi, σ_y = 57 ksi and El. = 6 % and represent the same drop relative to T6 properties. The elastic modulus of 2090 averaged over 16 tests was estimated to be 11.7 $\pm$ 0.25 Msi ($\approx$ 81 GPa).

Comparison of the strengthening behavior, in Figure 9, with the hardening behavior, in Figure 7(b), for 2090 reveals good agreement. The peak location for the T6 and T5/CWQ conditions (60 hrs) and the decrease in peak aging time for the T5/AAC condition (24-40 hrs) is common to both sets of data. It is observed that there is a progressive decrease in peak properties from the T6 to the T5/CWQ to the T5/AAC temper. The drop in maximum strength follows the decrease in peak hardness as a function of temper and the difference between the hardness and tensile data in the highly underaged condition is similar. The aging behavior documented is consistent with previous reports regarding the effect of thermal processing variables on properties of alloy 2090 [30,33,34].

As was the case for 8090, underaging will not result in a significant improvement in ductility, but 40 hrs at 350°F for T6 processing allows the ductility criterion to be satisfied. The peak aged conditions for both T5-type tempers already meet the criteria established for defining an underaging treatment, namely ductility and aging time. However, 2090 material is most frequently used in a slightly underaged condition as a result of better fracture toughness and corrosion behavior [8,25]. Therefore, from Figure 9, underaging for 16 hrs at 350°F appears appropriate for both the T5/CWQ and T5/AAC conditions. The post-SPF property data summarized for 2090 in Table VI reveals that eliminating SHT has a larger impact than removal of CWQ during post-SPF thermal processing. The yield strength is degraded more than the ultimate strength and similar to 8090 can be correlated with large increases in ductility [37].

The data suggest that elimination of SHT was primarily responsible for the degradation in properties observed. As noted in Table V, the temperature differential of 50°F between T_{SPF} and T_{SHT} is the greatest of the three alloys considered. As a result of this difference, this material is likely to be in a partially solution treated condition after forming. The significant drop in strength between the T6 and T5/CWQ tempers reflects a decrease in available solute and a reduction in the strengthening response during subsequent artificial aging [39]. Comparing the T5/AAC with the T6 temper data reveals a further decrease in strength and also a reduction in the peak aging time. It has been shown that slower cooling result in the formation of nucleation sites for intragranular precipitation [33,34]. Such an effect would account for the differences observed during the thermal processing studies conducted on the 2090 material.

The implication of the 2090 data presented is that the SHT step cannot be removed without degradation in post-SPF properties. However, it is noteworthy that the post-SPF properties compare favorably with the data for 8090. In a similar manner, increasing the

forming temperature, such that $T_{SPF} \approx T_{SHT}$, would result in a fully solution treated condition at the conclusion of forming. Uniaxial superplastic elongations in excess of 500% have been attained in 2090-OE16 in the temperature range of 985-1015°F (530-546°C) without back pressure [10,15,40]. It is anticipated that T5/CWQ properties much closer to T6 properties would result assuming adequate superplastic formability at the higher temperature. The absence of an appreciable change between the T5/CWQ and T5/AAC properties for the lower temperature suggests that it may also be possible to implement slower cooling.

3.3.3 Alloy X2095-RT72

The influence of temper/quench rate selection on the post-SPF strengthening behavior of X2095 during artificial aging at 350°F is presented in Figure 10. In contrast to the behavior observed in 8090 and 2090, there is evidence of a reversion in strengthening response after short-time artificial aging. In all three temper conditions, ductility is in the range of 15-20% in the highly underaged condition and decreases to 3-4% for peak strength. The peak is located at an aging time of 16-24 hrs and the difference in strength relative to the 1 hr aging data is substantially larger than that observed for either 8090 or 2090. Consequently, the strengthening response is much more rapid for this alloy and the associated drop in ductility is much larger. On comparing the strengthening behavior, in Figure 10, with the hardening behavior, in Figure 7(c), for X2095, the data are in close agreement. The strong response to artificial aging between 1 hr and peak is evident in both sets of data and is consistent with behavior noted elsewhere for superplastically formed X2095 material of similar vintage [17]. However, the exclusion of 0-1 hr aging data in this study precludes any reliable estimate of the extent of the reversion.

Figure 10(a) reveals that aging for maximum strength occurs following 16 hrs at 350°F for T6 processing and the peak properties consist of σ_u= 94 ksi, σ_y= 90 ksi and El.= 4 %. The data show that the peak aging time lengthens to 24 hrs at 350°F during processing for a T5-type temper. In Figure 10(b), for the T5/CWQ condition, the post-SPF properties at peak consist of σ_u= 97 ksi, σ_y= 95 ksi and El.= 3 %. These data actually represent an increase in strength with a decrease in ductility compared to the baseline condition. The reason for this anomalous behavior relative to the general trends in the data presented for post-SPF 8090 and 2090 materials is uncertain. The data for the T5/AAC temper in Figure 10(c), do conform to the property/ processing trends established. In contrast to the T5/CWQ condition, the peak values of σ_u= 82 ksi, σ_y= 71 ksi and El.= 4 % reveal a degradation in properties. These results represent a 13 percent drop in ultimate strength, a 20 percent decrease in yield strength, but no change in ductility compared to the T6 condition.

The value for the elastic modulus of X2095 was estimated to be 11.6 $\pm$ 0.25 Msi ($\approx$ 80 GPa) from 19 sets of tensile data. Although the data suggest that X2095 is somewhat quench sensitive, the alloy attains higher absolute strength in the T5/AAC condition than the other two alloys in the baseline T6 condition. The exceptional ductilities associated with the highly underaged condition indicate that X2095 has a decided advantage over 8090 and 2090 with respect to obtaining balanced properties. The trends in elongation data suggest that satisfactory improvements relative to the low, peak-aged ductility can be achieved for all three tempers.

However, the rapid decrease in ductility was not anticipated during the inception of the experimental matrix.

The absence of data between 3 and 10 hrs of aging at 350°F makes definition of a suitable underaging treatment difficult for the T6 and T5/CWQ conditions. The results show that an aging time of 3 hrs produces the desired ductility, but with too great a sacrifice in strength compared to the peak-aged values. In contrast, aging for 10 hrs does not result in a large decrease in strength, but the ductility is less than the prescribed minimum. The trends in the data suggest that the best balance between strength and ductility can be achieved by specifying an underaging time of 8 hrs. Underaged properties of $\sigma_u \approx$ 90 ksi, $\sigma_y \approx$ 80 ksi and for the T6 and T5/CWQ tempers were interpolated from the data presented for El. $\approx$ 5%. Acceptable ductility has been obtained by specifying an equivalent underaged condition in non-SPF processed material of similar composition [17,41].

Typical post-SPF tensile properties of the X2095 material included in this study are shown in Table VI. Comparing the T6 and T5/CWQ data reveals that the change in properties resulting from removal of the SHT step is negligible. As for 8090, this is probably a reflection of the small (15°F) temperature differential between T_{SPF} and T_{SHT} for X2095. Examination of the T5/AAC data shows that the drop in strengths is quite severe compared to the T6 baseline. Also, as documented for 8090 and 2090, the yield strength is apparently affected more than the ultimate strength by thermal processing modification. Removal of CWQ results in a larger degradation in properties than eliminating SHT in 0.6 SPF strain material. The data imply that the T5/CWQ condition would be the most appropriate temper for simplified post-SPF thermal processing of X2095.

At the forming temperature employed, SHT can be eliminated, but replacing CWQ with AAC appears to result in excessive degradation of properties. However, it may be possible to dispense with CWQ by using a cooling rate intermediate between CWQ and AAC. It is suggested that a slightly slower cooling rate than CWQ may suffice, such as the use of an aqueous glycol quenchant (GWQ). This is common industrial practice for reducing cooling rates while still achieving a satisfactory T5-type temper condition in Al alloys [42]. Further, a 25 vol.% GWQ would be appropriate for the sheet thicknesses characteristic of these particular SPF components. Another solution, similar to the case of 2090, may be to increase T_{SPF} so that slower cooling rates can be employed. The material will be in a fully solution treated condition at the conclusion of forming if $T_{SPF} \approx T_{SHT}$ is plausible based on formability. It has been demonstrated that uniaxial elongations of >600% while forming at 935-950°F (504-516°C), in the absence of back pressure, are attainable in X2095 [10,17,18].

4. CONCLUDING REMARKS

A direct comparison of the post-SPF mechanical properties of commercial superplastic Al-Li alloys was made possible by the systematic approach adopted. The data compiled reveal the extent to which post-SPF procedures can be simplified without sacrificing properties relative to T6 thermal processing. The T5/CWQ data show that SHT can be eliminated for processing of 8090 and X2095. The T5/AAC data for these two alloys shows that a cooling rate from the SPF die intermediate between CWQ and AAC is required. It is suggested that, for 8090, FAC to produce cooling marginally faster than AAC and for X2095, GWQ to produce cooling marginally slower than CWQ can be employed. In the case of 2090, the data reveal that SHT cannot be eliminated and also that the alloy is quench sensitive. However, comparison of the T5/CWQ with the T5/AAC data suggests that CWQ following SHT may not be necessary. Eliminating SHT for 8090 and X2095 will reduce the number of processing steps, whereas eliminating CWQ will improve component tolerances and reduce re-working requirements. These factors have the potential to add up to considerable cost savings compared to conventional manufacturing practices.

An important conclusion which may be drawn from the results concerns selection of appropriate SPF temperatures for Al-Li alloys. The data presented suggest that the optimum SPF temperature may not be the temperature at which maximum formability is attained per se, but the highest temperature at which the formability is still adequate. The higher forming temperature may permit the combination of SPF and post-SPF thermal processing to better substitute for formal solution heat treatment. It is clear that selecting $T_{SPF} \geq T_{SHT}$ will be beneficial to T5 processing from the perspective of retaining T6 properties while eliminating SHT and using AAC for all three alloys. Current information indicates that there is considerable flexibility with regards to the temperature range within which Al-Li components can be superplastically formed. Although the specific temperature will be dependent on the SPF strain required for complete formation of a specified component, higher SPF temperatures for 2090 and X2095 create the potential for further simplification of post-SPF procedures. The data presented suggest that, even though these two alloys are more quench sensitive than 8090, the degradation in properties can be restricted to acceptable margins.

It is important to note that any recommendations concerning the use of T5-type tempers for superplastically formed components must consider the SPF temperature employed. The results of this investigation reflect the use of forming temperatures which produced the optimum superplastic response for the individual alloys. Of the aging temperatures considered, 350°F was the best for all three Al-Li alloys from the perspective of achieving peak-aged properties using aging times of $\leq$ 40 hrs. It is not inferred that this is the optimum aging temperature, but the slightly underaged tensile properties documented meet, or exceed, data reported from other sources. It should be stressed that one objective of this study was that the data compiled be representative of bulk material. Any comparison with these data must consider that higher levels of SPF strain or the presence of solute-depleted surfaces may influence material performance.

In this investigation, defining a uniform starting condition for the materials was aimed at facilitating comparison of the data with other sources. In general, alloy composition and thermomechanical treatment to superplastic sheet will determine the as-received condition of the material. Subsequently, the SPF parameters used, such as temperature, strain rate, back pressure (cavitation suppression) and the level of deformation required to produce a particular component geometry will control the as-formed condition. Differences in grain size and texture resulting from differing SPF strain will tend to have an impact on both aging response and mechanical properties. It is anticipated that the attention to detail concerning data compilation may prove beneficial for establishing a post-SPF mechanical property database in the future.

5. ACKNOWLEDGEMENTS

This work was conducted in support of the Advanced Launch Systems Development Program in the Materials Division at NASA Langley Research Center with Mr. Thomas T. Bales as technical monitor. Mr. H.E. Lippard gratefully acknowledges the support of the Langley Aerospace Research Summer Scholar program 1990-92. The authors wish to thank Mr. J.A. Wagner and Mr. O.R. Singleton for their careful reviews of this manuscript.

6. REFERENCES

1. S.J. Hales and J.A. Wagner: "Superplastic Forming of Al-Li Alloys for Lightweight, Low-cost Structures", in ***Technology 2000***, NASA Conference Publication 3109, vol. 2, 1991, pp. 200-209.
2. J.A. Wagner, S.J. Hales and W.F. James: ***"Superplastic Forming of Built-up Structures"***, presented at the AeroMat '91 Conference, ASM International, Long Beach, CA, May 20-24, 1991.
3. D. Stephen: "Designing for Superplastic Alloys", in ***Superplasticity***, NATO/AGARD-LS-168, SPS Ltd., England, 1989, pp. 7.1-7.37.
4. J.E. Hatch (Ed.): "Metallurgy of Heat Treatment and General Principles of Precipitation Hardening", in ***Aluminum: Properties and Physical Metallurgy***, ASM, Metals Park, OH, 1984, pp. 134-143.
5. D.S. Thompson, O.R. Singleton, R.D. McGowan and G.E. Spangler: "Heat-treatable Aluminium Alloys and Heat-treating Techniques", J. Scientific & Industrial Research, vol. 29, no. 5, 1970, pp. 219-231.
6. B.J. Dunwoody and R.J. Stracey: "Superplastic Forming of Aluminium Alloys", J. Metals and Materials, vol. 5, no. 8, 1989, pp. 464-467.
7. S. Fox, H.M. Flower and D.S. McDarmaid: "Formation of Solute-depleted Surfaces in Al-Li-Cu-Mg-Zr Alloys and Their Influence on Mechanical Properties", in ***Aluminium-Lithium Alloys III***, C. Baker, P.J. Gregson, S.J. Harris and C.J. Peel, eds., The Institute of Metals, London, 1986, pp. 263-272.

8. A. Roth and H. Kaesche: "Electrochemical Investigation of Technical Aluminum-Lithium Alloys - Part II", in ***Aluminum-Lithium Alloys V***, T.H. Sanders and E.A. Starke, eds., MCEP Ltd., England, vol. III, 1989, pp. 1207-1216.
9. A.J. Shakesheff, D.S. McDarmaid and P.J. Gregson: "Effect of Microstructure on Tensile and Fatigue Properties of Superplastically Formed Al-Li-Cu-Mg-Zr 8090 Alloy Sheet", J. Mater. Sci. Tech., vol. 7, no. 3, 1991, pp. 276-281.
10. A.K. Ghosh and C.H. Hamilton: "Forming of a Long Rectangular Box Section - Analysis and Experiment", in ***Process Modeling - Fundamentals and Applications to Metals***, ASM, Metals Park, OH, 1978, pp. 303-331.
11. S.J. Hales, T.T. Bales, W.F. James and J.M. Shinn: "Fabrication of Structural Components from Commercial Aluminum Alloys Using Superplastic Forming", in ***Superplasticity in Aerospace II***, T.R. McNelley and H.C. Heikkenen, eds., TMS, Warrendale, PA, 1990, pp. 167-185.
12. J.M. Papazian, R.L. Schulte and P.N. Adler: "Lithium Depletion During Heat Treatment of Aluminum-Lithium Alloys", Metall. Trans. A, vol. 17A, no. 4, 1986, pp. 635-643.
13. R. Amichi and N. Ridley: "Superplastic Behavior and Microstructural Evolution in Al-Li Alloy 8090 (LITAL A)", in ***Aluminum-Lithium Alloys V***, T.H. Sanders and E.A. Starke, eds., MCEP Ltd., England, vol. I, 1989, pp. 159-167.
14. T. Tsuzuku and A. Takahashi: "Superplastic Forming Under Hydrostatic Pressure and Heat Treatments in an Al-Li Alloy", J. Jap. Inst. Light Metals, vol. 39, no. 11, 1989, pp. 824-830.
15. C.C. Bampton, B.A. Cheney, A. Cho, A.K. Ghosh and C. Gandhi: "Superplastic Forming of Aluminum-Lithium Alloy 2090-OE16", in ***Superplasticity in Aerospace***, H.C. Heikkenen and T.R. McNelley, eds., TMS-AIME, Warrendale, PA, 1988, pp. 247-259.
16. M.J. Reynolds, C.A. Henshall and J. Wadsworth: "Superplastic Forming Characteristics and Properties of Aluminum-Lithium Sheet Alloys", in ***Aluminum-Lithium Alloys: Design, Development and Application Update***, R.J. Kar, S.P. Agrawal and W.E. Quist, eds., ASM International, Metals Park, OH, 1988, pp. 357-399.
17. P.J. Smith-Hartley, K.S. Kumar and S.A. Brown, "The Effects of Processing Parameters on the Post-SPF Microstructure and Mechanical Properties of Weldalite^{TM}049", in ***Advances in Superplasticity and Superplastic Forming***, N. Chandra, R.E. Goforth and H. Garmestani, eds., TMS, Warrendale, PA, 1993.
18. B.-T. Ma and J.R. Pickens: ***"Superplastic Formability of Al-Cu-Li Alloy Weldalite^{TM}049"***, NASA Contractor Report 4367, Martin Marietta Laboratories, Baltimore, MD, May 1991.
19. ***Annual Book of Standards; Metals - Mechanical Testing***, ASTM, Philadelphia, PA, vol. 3.01, 1989, pp. 469-477.
20. ***Annual Book of Standards; Metals - Mechanical Testing***, ASTM, Philadelphia, PA, vol. 3.01, 1989, pp. 177-182.
21. ***Annual Book of Standards; Metals - Mechanical Testing***, ASTM, Philadelphia, PA, vol. 3.01, 1989, pp. 50-53.

22. J.M. Papazian, G.G. Bott and P. Shaw: "Effects of Lithium Loss on Strength and Formability of Aluminum-Lithium Alloys 8090 and 2090", Mater. Sci. Engng., vol. 94, no. 2, 1987, pp. 219-224.
23. J.M. Papazian and R.L. Schulte: "Lithium Diffusion in Aluminum-Lithium Alloy 2090 Clad With 7072", Metall. Trans. A, vol. 21A, no. 1, 1990, pp. 39-43.
24. E.A. Starke and W.E. Quist: "The Microstructure and Properties of Aluminum-Lithium Alloys", in ***New Light Alloys***, NATO/AGARD-LS-174, SPS Ltd., England, 1990, pp. 2.1-2.21.
25. W.G.J. 't Hart, L. Schra, D.S. McDarmaid and M. Peters: "Mechanical Properties and Fracture Toughness of 8090-T651 Plate and 2091 and 8090 Sheet", in ***New Light Alloys***, NATO/AGARD-CP-444, SPS Ltd., England, 1989, pp. 5.1-5.17.
26. F.W. Gayle, F.H. Heubaum and J.R. Pickens: "Natural Aging and Reversion Behavior of Al-Cu-Li-Ag-Mg Alloy Weldalite 049", in ***Aluminum-Lithium Alloys V***, T.H. Sanders and E.A. Starke, eds., MCEP Ltd., England, vol. II, 1989, pp. 701-710.
27. K.S. Kumar, S.A. Brown and J.R. Pickens: "Effect of a Prior Stretch on the Aging Response of an Al-Cu-Li-Ag-Mg Alloy", Scripta Metall. Mater., vol. 24, no. 7, 1990, pp. 1245-1250.
28. F.W. Gayle, F.H. Heubaum and J.R. Pickens: "Structure and Properties During Aging of a Ultra-High-Strength Al-Cu-Li-Ag-Mg Alloy", Scripta Metall. Mater., vol. 24, no. 1, 1990, pp. 79-84.
29. R.E. Goforth, M. Srinivasan, N. Chandra and L. Douskos: "Superplastic Flow Characteristics and Microstructural Analysis of Aluminum-Lithium Alloy 2090-OE16", in ***Superplasticity in Aerospace II***, T.R. McNelley and H.C. Heikkenen, eds., TMS, Warrendale, PA, 1990, pp. 285-302.
30. J.E. Hatch (Ed.): "Metallurgy of Heat Treatment and General Principles of Precipitation Hardening", in ***Aluminum: Properties and Physical Metallurgy***, ASM, Metals Park, OH, 1984, pp. 157-175.
31. W.S. Miller and J. White: "The Development of Superplastic 8090 and 8091 Sheet", in ***Superplasticity in Aerospace***, H.C. Heikkenen and T.R. McNelley, eds., TMS-AIME, Warrendale, PA, 1988, pp. 211-228.
32. R.G. Butler and B.J. Dunwoody: "Superplastic Performance and Properties of LITAL Alloys", in ***New Light Alloys***, NATO/AGARD-CP-444, SPS Ltd., England, 1989, pp. 17.1-17.7.
33. M.E. Donnellan and W.E. Frazier: "An Examination of the Quench Sensitivity of Alloy 2090", in ***Aluminum-Lithium Alloys V***, T.H. Sanders and E.A. Starke, eds., MCEP Ltd., England, vol. I, 1989, pp. 355-364.
34. M.E. Donnellan and W.E. Frazier: ***"Quench Sensitivity in Al-Cu-Li Alloys"***, Final Report 89046-60, Naval Air Development Center, Warminster, PA, February 1989.
35. R.S. James: "Aluminum-Lithium Alloys", in ***Metals Handbook***, 10th ed., ASM International, Metals Park, OH, vol. 2, 1990, pp. 178-199.
36. C.E. Anton, P. Rasmussen, C. Thompson, R. Latham, C.H. Hamilton, B. Ren, C. Gandhi and D. Hardwick: ***"Low Cost, SPF Aluminum Cryogenic Tank Structure for ALS"***, NASA Contractor Report 189654, Rockwell International - North American Aircraft, Downey, CA, May 1992.

37. D.S. McDarmaid and A.J. Shakesheff: "The Effect of Superplastic Deformation on the Tensile and Fatigue Properties of Al-Li (8090) Alloy", in ***Proc. 4th Int. Al-Li Conf.***, G. Champier, B. Dubost, D. Mianney and L. Sabetay, eds., J. de Physique, France, vol. 48, no. 9, C3, 1987, pp. 257-268.
38. J.A. Wagner: "Age Hardening Characteristics and Mechanical Behavior of Al-Cu-Li-Zr-In Alloys", in ***Light-Weight Alloys for Aerospace Applications***, E.W. Lee, E.H. Chia and N.J. Kim, eds., TMS, Warrendale, PA, 1989, pp. 221-233.
39. W.E. Quist and G.H. Narayanan: "Aluminum-Lithium Alloys", in ***Aluminum Alloys - Contemporary Research and Applications***, A.K. Vasudevan and R.D. Doherty, eds., Treatise on Materials Science and Technology, Academic Press, San Diego, CA, vol. 31, 1989, pp. 219-254.
40. C.W. Cho, B.A. Cheney, D.J. Lege and J.I. Petit: "Superplasticity of 2090 Sheet at Hot Rolled Gauge", in ***Proc. 4th Int. Al-Li Conf.***, G. Champier, B. Dubost, D. Mianney and L. Sabetay, eds., J. de Physique, France, vol. 48, no. 9, C3, 1987, pp. 277-283.
41. J.R. Pickens, F.H. Heubaum, T.J. Langan and L.S. Kramer: "Al-(4.5-6.3)Cu-1.3Li-0.4Ag-0.4Mg-0.14Zr Alloy Weldalite^{TM}049", in ***Aluminum-Lithium Alloys V***, T.H. Sanders and E.A. Starke, eds., MCEP Ltd., England, vol. III, 1989, pp. 1397-1414.
42. O.R. Singleton, "An Analysis of New Quenchants for Aluminum", J. Metals, vol. 20, no. 11, 1968, pp. 60-67.

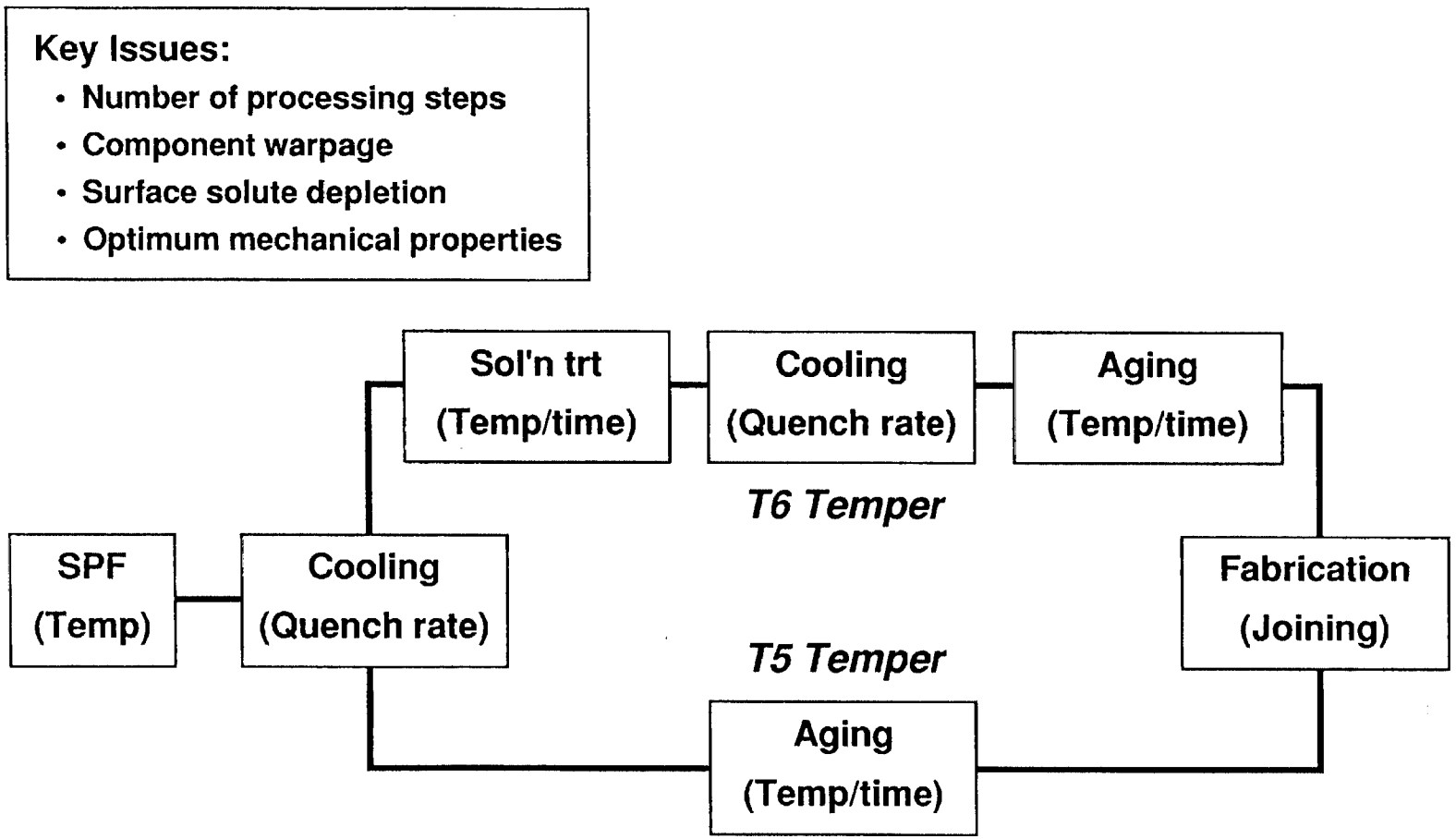

Figure 1. A schematic diagram which illustrates the different post-SPF thermal processing procedures which can be employed. The key issues associated with replacing T6 processing with T5-type processing are highlighted.

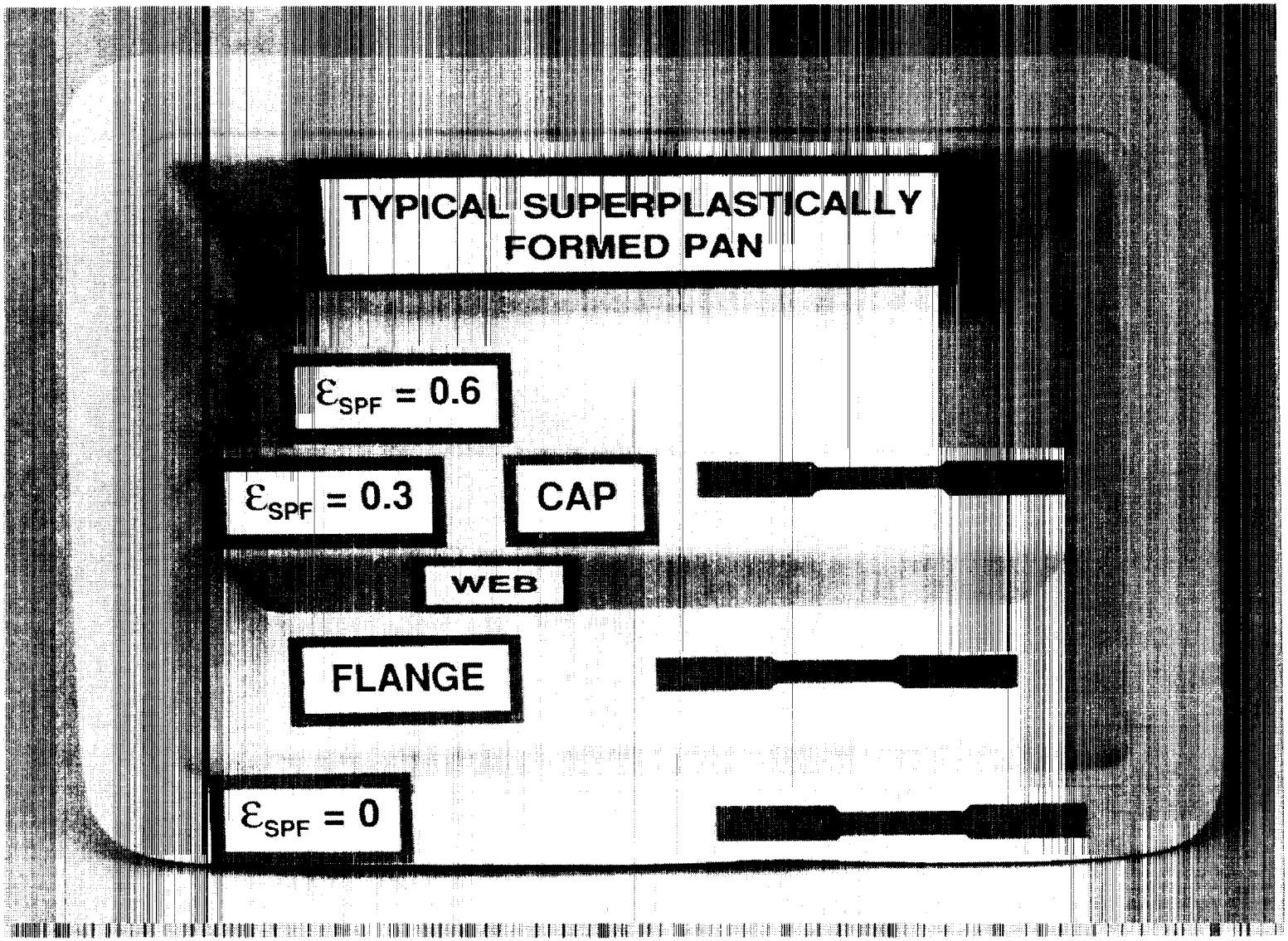

Figure 2. A superplastically formed Al-Li alloy component which has been partially trimmed for demonstration purposes is shown. The structural elements of the 0.2 m long, 'top-hat' stiffener, in conjunction with the nominal level of SPF strain characteristic of the three different regions, are indicated. The locations and orientation of tensile blanks which could be extracted for post-SPF thermal processing studies are identified.

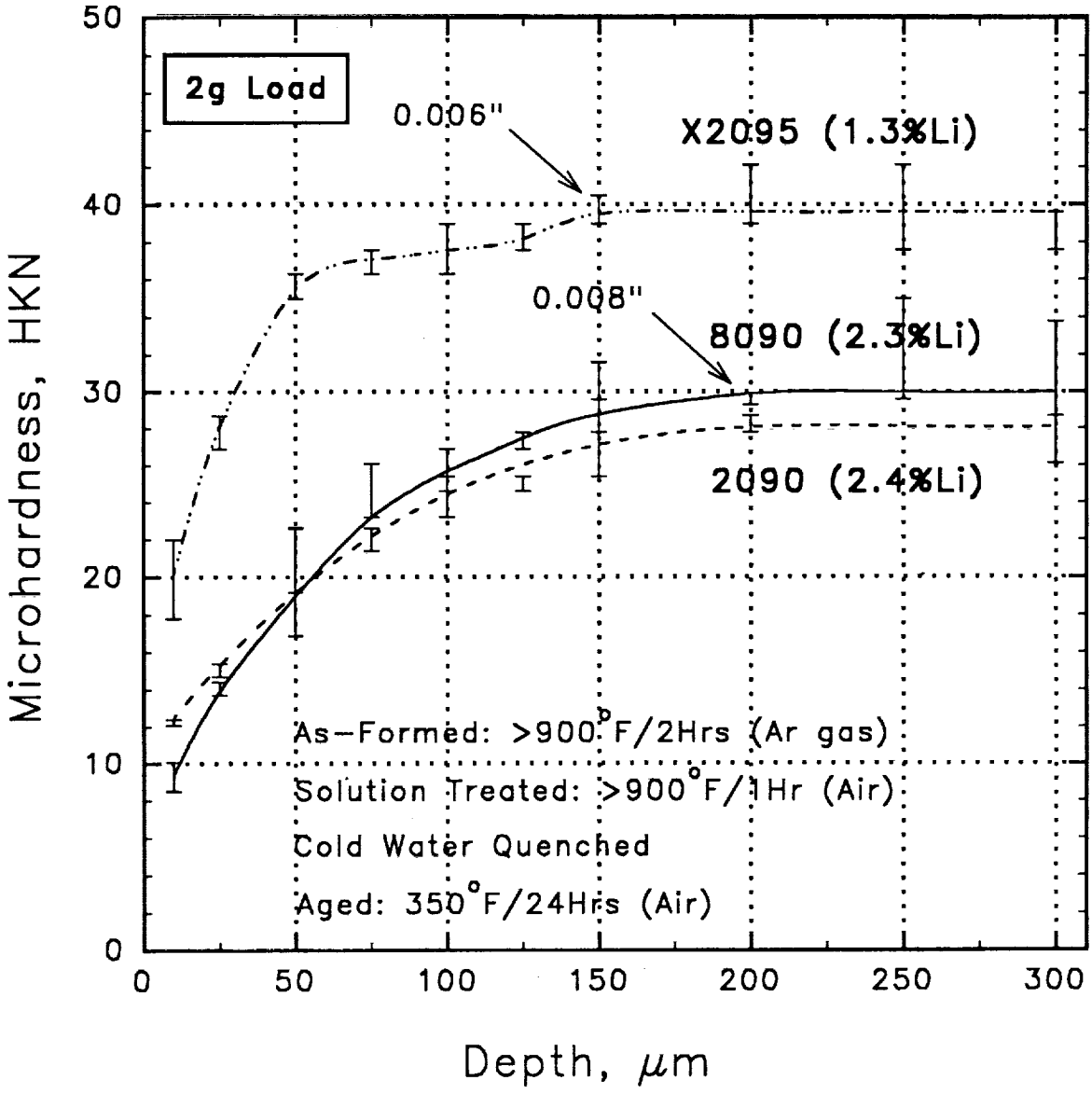

Figure 3. Profile of microhardness as a function of depth from the surface for sheet material biaxially deformed to a superplastic strain of 65% (0.5) and thermally processed to an approximate T6 temper condition.

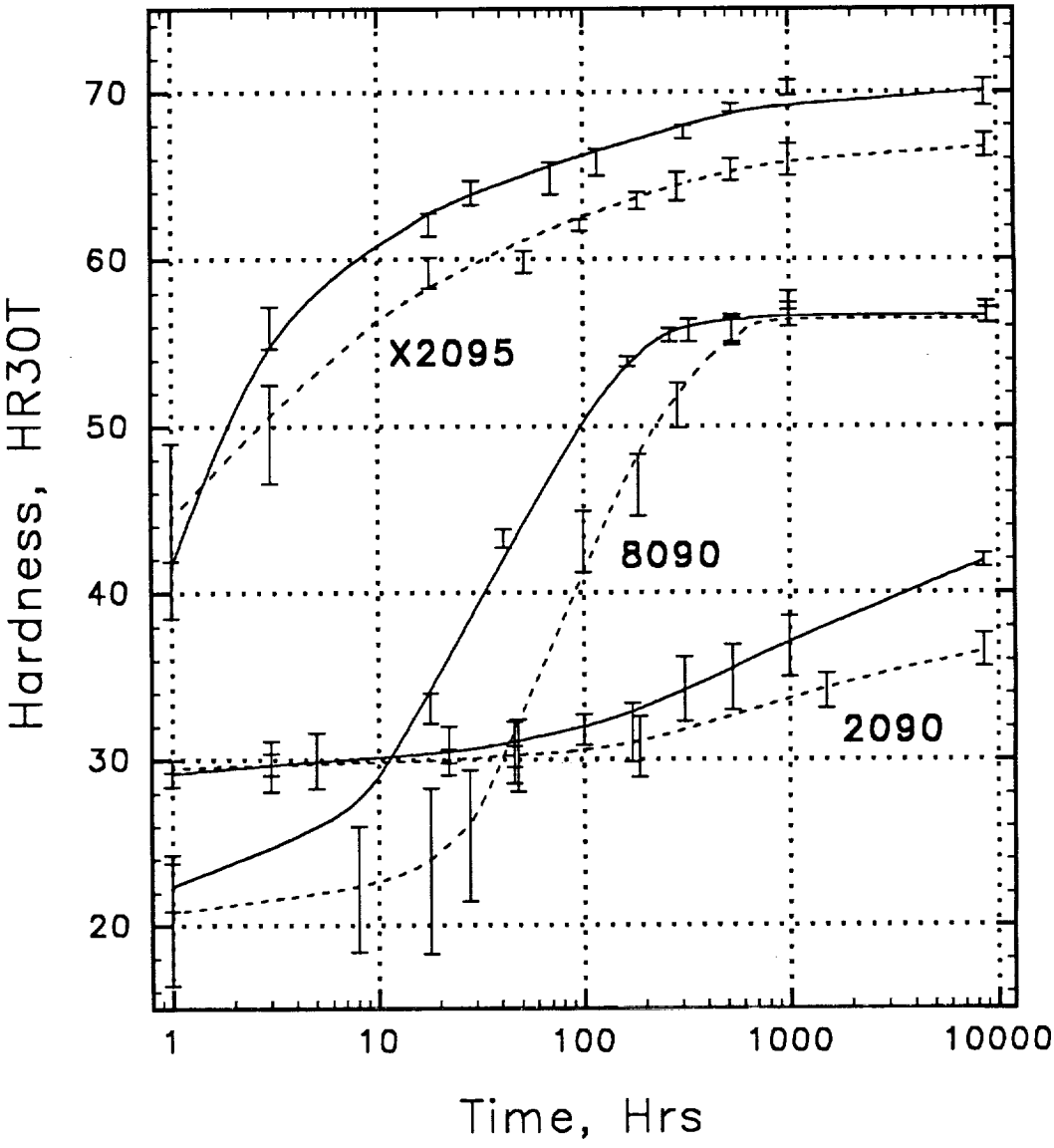

Figure 4. Natural aging behavior of material deformed to a superplastic strain of 80% (0.6) followed by Cold Water Quenching (——) or Accelerated Air Cooling (------) from the SPF temperature.

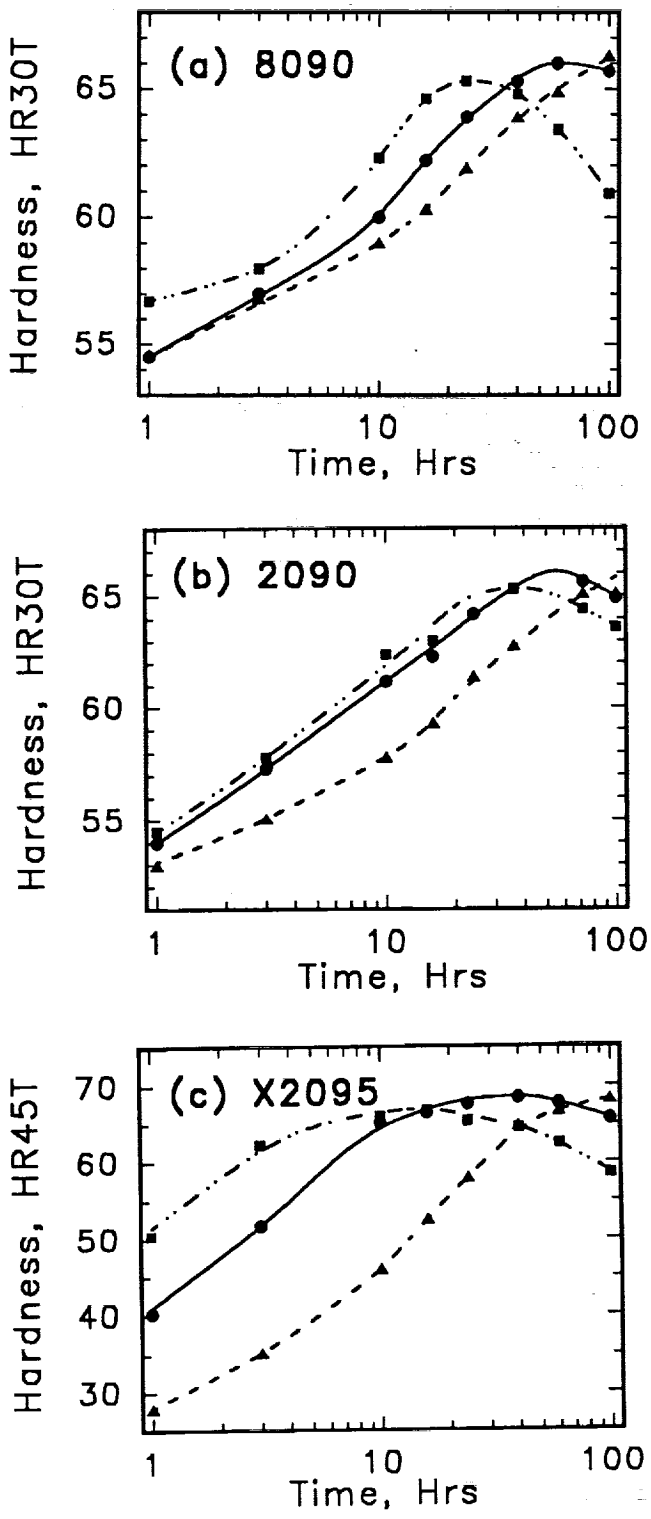

Figure 5. Hardening behavior as a function of aging temperature in 80% (0.6) SPF strain material for :- (a) 8090; (b) 2090; (c) X2095. The materials were cold water quenched from the SPF temperature followed by aging at :- 163°C/325°F (▲); 177°C/350°F (●); 191°C/375°F (■).

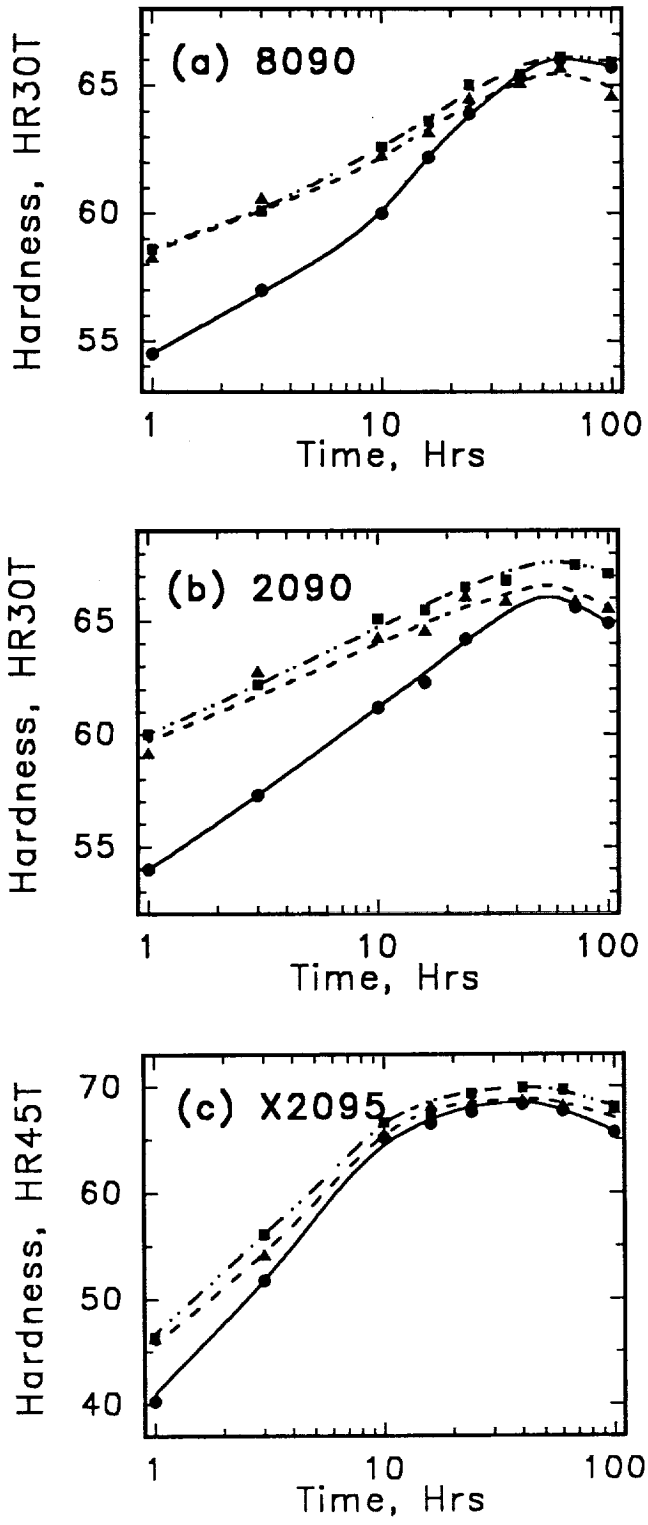

Figure 6. Hardening behavior as a function of superplastic strain while aging at 177°C/350°F for :- (a) 8090; (b) 2090; (c) X2095. The materials were cold water quenched from the SPF temperature following deformation to a superplastic strain of :- 0 (▲); 35%/0.3 (■); 80%/0.6 (●).

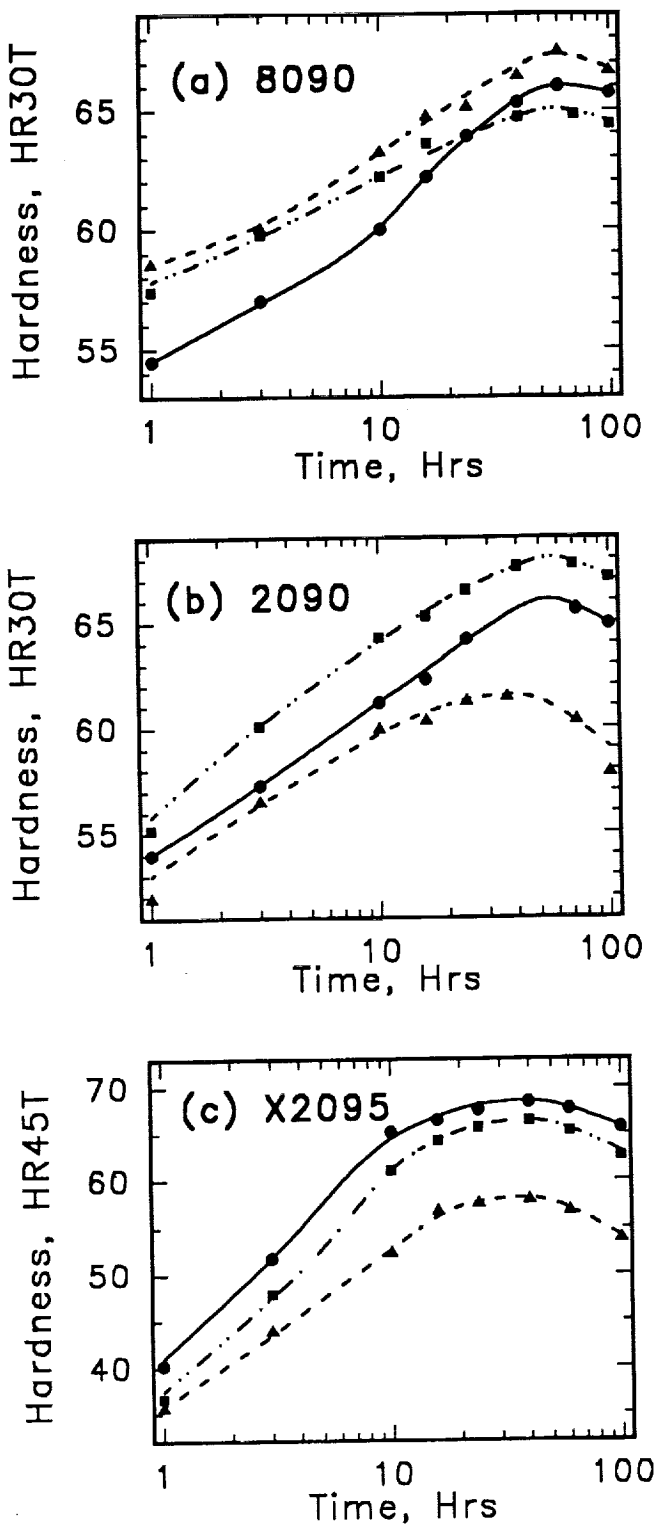

Figure 7. Hardening behavior as a function of temper/quench rate selection in 80% (0.6) SPF strain material for :- (a) 8090; (b) 2090; (c) X2095. The materials were aged at 177°C/350°F to the following tempers :- T6/CWQ (■); T5/CWQ (●); T5/AAC (▲).

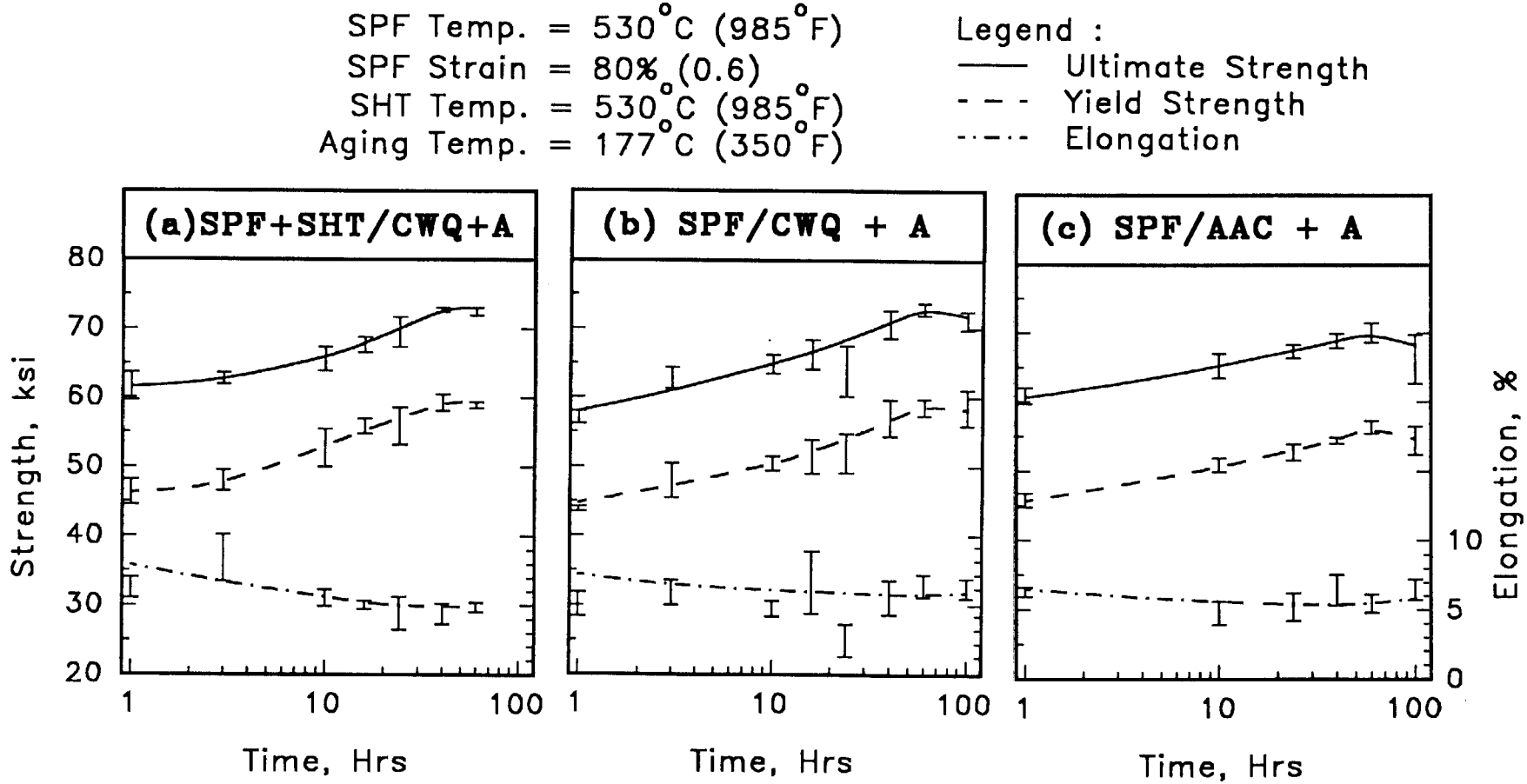

Figure 8. The effect of post-SPF thermal processing on the strengthening response of Al-Li alloy 8090. The data are presented as a function of temper/quench rate selection for :- (a) T6/CWQ; (b) T5/CWQ; (c) T5/AAC.

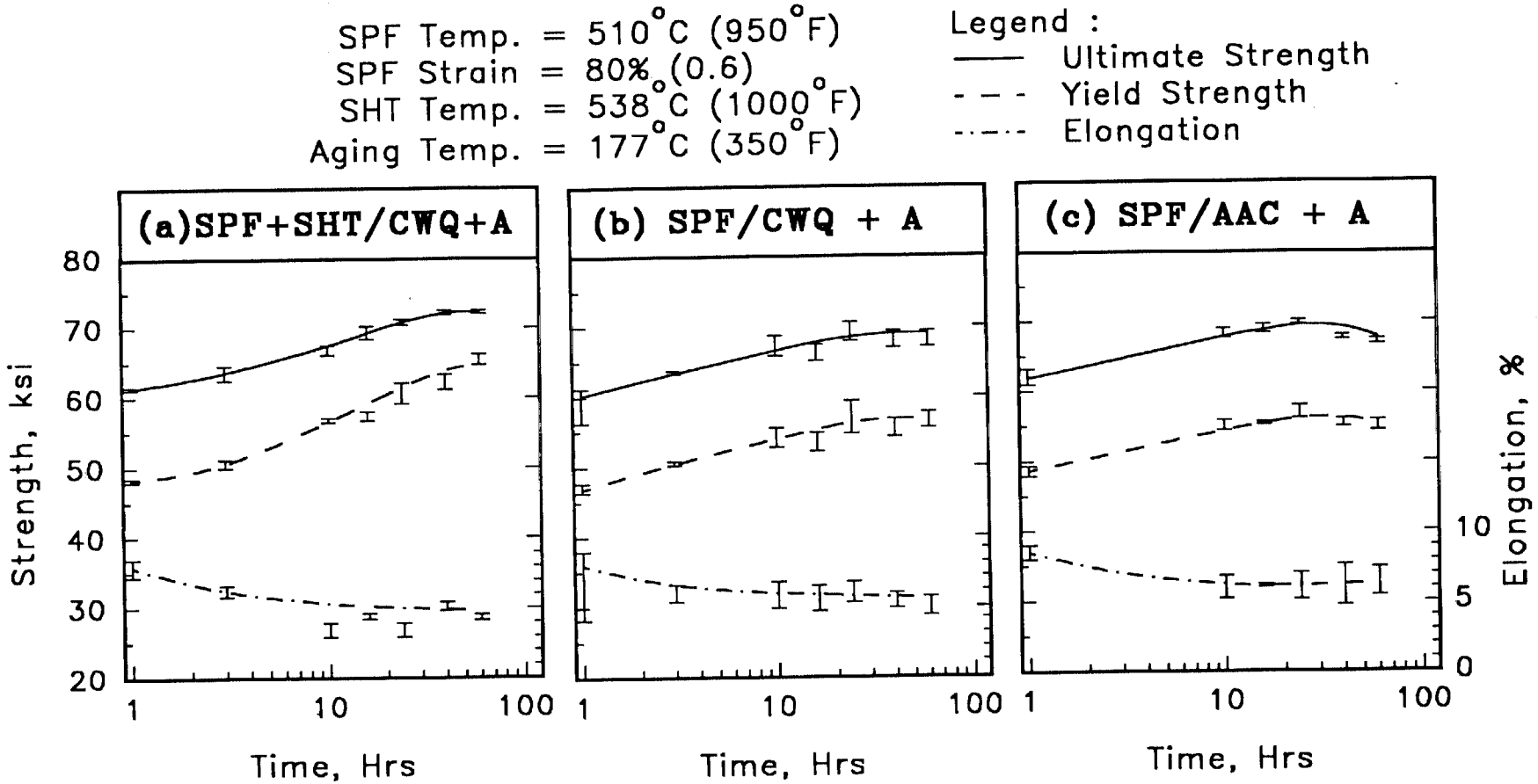

Figure 9. The effect of post-SPF thermal processing on the strengthening response of Al-Li alloy 2090. The data are presented as a function of temper/quench rate selection for :- (a) T6/CWQ; (b) T5/CWQ; (c) T5/AAC.

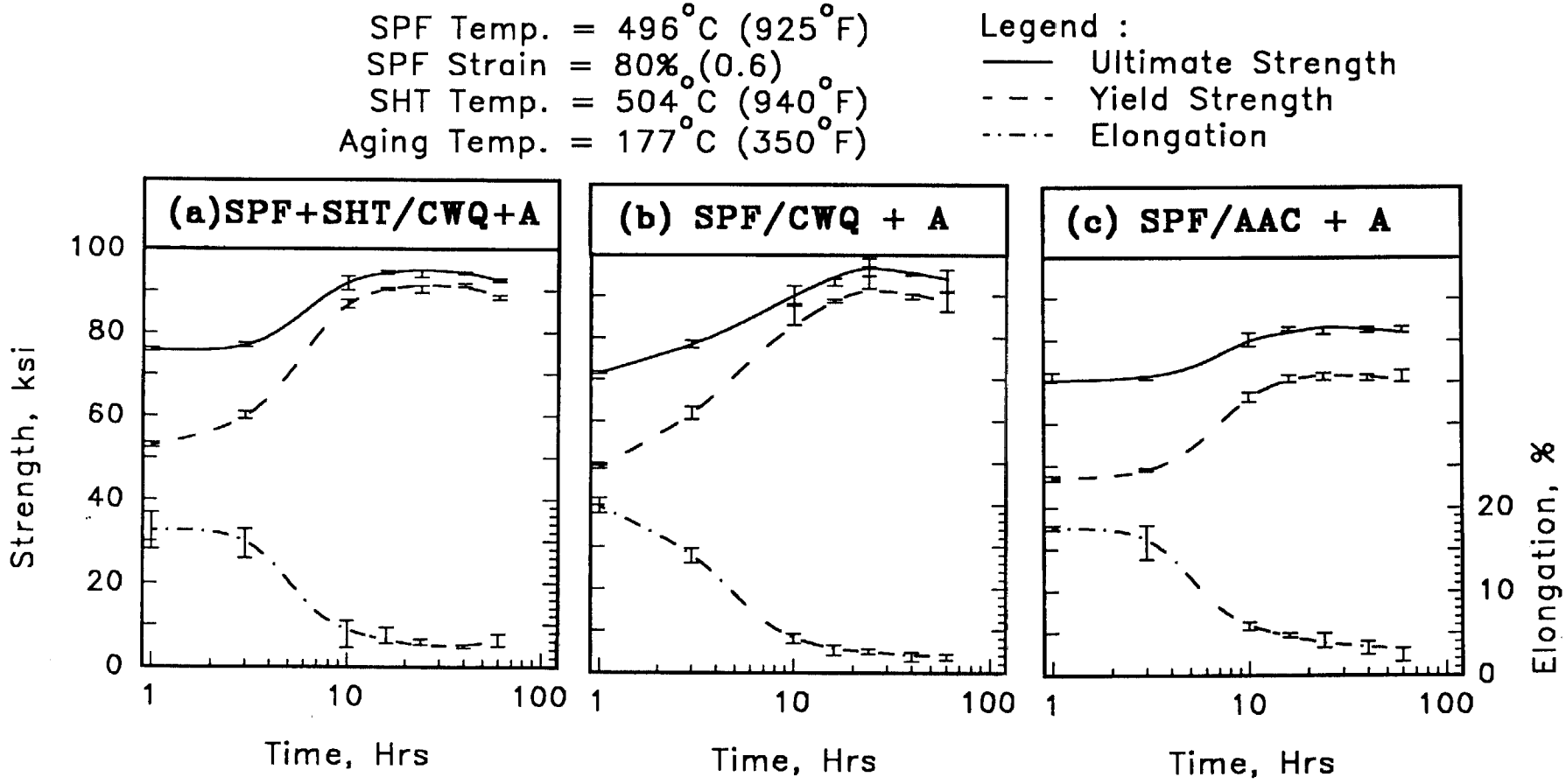

Figure 10. The effect of post-SPF thermal processing on the strengthening response of Al-Li alloy X2095. The data are presented as a function of temper/quench rate selection for :- (a) T6/CWQ; (b) T5/CWQ; (c) T5/AAC.

APPENDIX

X2095

Table A1. Natural aging response following SPF for material deformed to 0.6 strain.

ALLOY	Cold Water Quenched				Accelerated Air Cooled			
	Time (Hrs)	Hardness (HR30T)			Time (Hrs)	Hardness (HR30T)		
		High	Low	Avg.		High	Low	Avg.
8090	1	23.8	20.9	22.4	1	24.3	16.4	20.8
	--	--	--	--	8	26.0	18.4	22.9
	18	34.0	32.2	32.9	18	28.3	18.3	24.3
	--	--	--	--	28	29.4	21.5	26.1
	41	43.8	42.7	43.3	48	32.4	28.1	30.3
	165	54.2	53.6	53.9	100	44.9	41.2	42.5
	264	55.9	55.1	55.5	185	48.3	44.6	46.5
	328	56.4	55.1	55.8	289	52.6	49.9	51.4
	528	56.7	55.1	56.0	528	56.5	54.9	55.8
	1000	58.1	57.0	57.4	1000	57.4	56.0	56.5
	8904	57.1	56.2	56.6	8884	57.5	56.2	56.7
2090	1	30.0	28.4	29.2	1	30.0	29.3	29.7
	3	31.1	29.1	30.3	3	30.4	28.1	29.5
	5	31.6	28.3	29.7	--	--	--	--
	22	32.0	29.1	31.0	22	30.6	29.8	30.0
	46	32.3	28.6	31.1	46	30.8	29.6	30.1
	100	32.7	30.9	31.9	--	--	--	--
	172	33.4	29.9	31.6	186	32.6	29.0	31.1
	309	36.2	32.3	34.4	--	--	--	--
	530	36.9	33.0	35.0	--	--	--	--
	1000	38.6	35.0	37.5	1500	35.2	33.1	34.3
	8572	42.3	41.5	41.9	8568	37.6	35.6	36.5
X2095	1	41.9	38.5	40.0	1	49.0	38.5	44.7
	3	57.2	54.7	55.9	3	52.5	46.6	50.4
	18	62.8	61.4	62.2	18	60.1	58.3	59.3
	29	64.7	63.3	63.9	52	60.5	59.2	59.9
	70	65.8	63.9	64.9	97	62.4	61.7	62.0
	118	66.6	65.0	65.8	185	64.0	63.0	63.3
	311	68.0	67.2	67.5	289	65.2	63.5	64.4
	528	69.3	68.8	69.2	530	66.0	64.7	65.4
	1000	70.7	69.8	70.1	1000	66.9	65.0	65.9
	8760	70.8	69.2	70.0	8765	67.5	66.1	66.7

Table A2. Age hardening behavior of 8090 as a function of temperature and SPF strain (ϵ) for material Cold Water Quenched following forming for a T5 temper. Units: Rockwell Superficial Hardness (30T scale).

Temp. (°F)	Time (Hrs)	ϵ = 0			ϵ = 0.3			ϵ = 0.6		
		High	Low	Avg.	High	Low	Avg.	High	Low	Avg.
325	1	59.0	56.0	57.7	60.4	55.7	58.3	55.1	53.9	54.6
	3	60.8	58.7	59.8	62.4	57.2	59.6	58.4	54.8	56.8
	10	62.8	60.0	61.4	63.7	60.1	62.0	59.6	58.1	59.0
	16	63.5	61.8	62.4	65.8	61.0	63.3	61.4	59.4	60.3
	24	65.3	61.6	63.7	65.3	63.3	64.0	62.8	61.1	61.9
	40	66.4	62.8	64.5	65.6	63.6	64.8	65.3	62.1	63.9
	60	65.3	64.4	64.9	66.2	63.5	65.4	65.9	64.1	64.9
	100	66.0	64.8	65.1	66.9	65.6	66.2	66.9	65.3	66.3
350	1	59.1	57.7	58.3	59.9	57.3	58.6	55.9	53.9	54.5
	3	63.9	57.7	60.6	62.5	57.0	60.1	58.5	55.6	57.0
	10	64.4	60.6	62.3	63.7	60.7	62.6	60.9	59.2	60.0
	16	65.2	62.2	63.2	66.2	62.4	63.6	63.7	61.1	62.2
	24	65.8	63.3	64.5	66.2	64.0	65.0	65.4	62.0	63.9
	40	66.0	64.1	65.1	66.0	64.8	65.4	66.8	64.2	65.3
	60	66.9	64.1	65.7	66.9	65.0	66.1	67.2	65.2	66.0
	100	65.9	63.5	64.6	67.1	63.7	65.9	67.2	65.2	65.7
375	1	60.2	56.5	58.5	62.9	58.4	60.6	57.7	55.6	56.7
	3	62.3	59.6	61.2	62.4	60.1	61.3	59.2	57.0	58.0
	10	64.9	63.5	64.4	65.6	61.4	63.4	63.1	60.6	62.3
	16	65.4	64.5	64.9	64.8	63.3	64.2	65.2	63.0	64.6
	24	66.9	64.5	65.6	66.9	65.1	65.9	66.6	63.8	65.3
	40	65.9	62.3	64.0	67.5	64.3	65.8	66.5	63.6	64.8
	60	63.7	61.1	62.5	66.3	63.2	64.8	64.2	62.7	63.4
	100	63.4	60.5	61.9	66.3	62.6	64.1	62.6	59.6	60.9

Table A3. Age hardening behavior of 8090 as a function of temperature and SPF strain (ϵ) for material Accelerated Air Cooled following forming for a T5 temper. Units: Rockwell Superficial Hardness (30T scale).

Temp. (°F)	Time (Hrs)	ϵ = 0			ϵ = 0.3			ϵ = 0.6		
		High	Low	Avg.	High	Low	Avg.	High	Low	Avg.
325	1	60.9	59.9	60.6	61.2	59.4	60.1	57.7	55.8	56.8
	3	63.1	61.4	62.4	61.7	61.2	61.4	59.1	57.4	58.2
	10	65.0	63.9	64.6	63.8	63.4	63.5	62.4	61.6	61.9
	16	66.1	65.0	65.6	65.5	64.3	64.9	63.8	62.9	63.4
	24	66.3	65.9	66.1	65.9	64.6	65.3	64.8	62.7	64.0
	40	66.9	66.1	66.6	67.0	65.8	66.3	66.2	64.3	65.0
	60	67.4	66.9	67.2	67.2	66.3	66.9	66.9	65.9	66.3
	100	67.7	67.4	67.5	68.8	68.2	68.4	68.3	67.4	67.9
350	1	60.8	59.6	60.2	62.6	61.5	62.0	59.4	57.8	58.6
	3	63.7	62.3	62.9	64.4	63.2	63.7	61.4	59.0	60.1
	10	65.5	65.1	65.3	65.7	64.8	65.2	63.8	62.8	63.3
	16	67.5	65.0	65.7	67.0	66.2	66.5	65.3	63.9	64.8
	24	67.1	65.7	66.4	67.5	66.1	66.9	65.7	64.8	65.2
	40	67.9	67.1	67.6	68.9	66.8	67.6	67.0	65.9	66.5
	60	68.1	67.4	67.8	68.5	68.2	68.4	68.4	66.7	67.5
	100	67.6	66.8	67.2	68.4	67.5	67.9	67.7	66.2	66.7
375	1	61.3	59.4	60.5	61.8	60.8	61.4	59.8	57.8	59.0
	3	64.2	63.2	63.6	63.9	63.0	63.5	62.6	61.9	62.2
	10	65.8	65.1	65.3	65.9	64.9	65.3	66.1	64.7	65.3
	16	66.9	65.2	66.2	67.5	66.0	67.0	67.8	65.1	66.0
	24	67.0	65.3	65.9	68.4	66.5	67.3	67.2	66.5	66.8
	40	63.7	62.8	63.1	66.5	65.7	66.1	65.7	64.5	65.2
	60	62.3	61.2	61.6	64.8	64.2	64.6	64.2	62.9	63.7
	100	58.4	56.7	57.5	61.0	59.9	60.5	57.0	56.6	56.8

Table A4. *Strengthening response of 8090 as a function of aging at 350°F for a T6 temper. (The starting material was deformed to 0.6 SPF strain, air cooled, Solution Heat Treated, cold water quenched and naturally aged 100 hours.)*

Aging Time (Hrs)	Hardness (HR30T)			Ult. Tens. Strength (ksi)			Yield Strength (ksi)			Elongation (%)			# of tests
	High	Low	Avg.	High	Low	Avg.	High	Low	Avg.	High	Low	Avg.	
1	58.0	56.5	57.4	63.6	59.6	61.6	48.1	44.5	46.3	7.0	5.5	6.2	2
3	61.0	58.6	59.8	63.6	61.9	62.8	49.5	46.5	47.9	10.1	6.7	8.1	3
10	63.9	60.5	62.2	67.3	63.9	65.9	55.4	50.0	52.8	6.1	4.9	5.7	3
16	64.9	61.9	63.6	68.8	66.5	67.8	57.0	54.8	55.6	5.3	4.7	5.0	3
24	65.0	64.1	64.6	71.7	67.3	69.8	58.6	53.2	56.8	5.6	3.2	4.7	5
40	66.2	63.9	64.7	73.0	72.4	72.7	60.5	58.1	59.3	5.1	3.6	4.4	2
60	65.8*	63.4*	64.8*	73.0	71.9	72.4	59.4	58.5	59.0	5.2	4.5	4.9	2
100	65.9	62.9	64.4	--	--	--	--	--	--	--	--	--	--

* *70 hour hardness data*

Table A5. Strengthening response of 8090 as a function of aging at 375°F for a T6 temper. (The starting material was deformed to 0.6 SPF strain, air cooled, Solution Heat Treated, cold water quenched and naturally aged 100 hours.)

Aging Time (Hrs)	Hardness (HR30T)			Ult. Tens. Strength (ksi)			Yield Strength (ksi)			Elongation (%)			# of tests
	High	Low	Avg.	High	Low	Avg.	High	Low	Avg.	High	Low	Avg.	
1	59.7	56.5	58.5	+0.2	-0.2	62.2	+0.2	-0.2	47.2	+0.2	-0.2	6.4	1
3	62.9	59.2	61.0	63.4	63.0	63.2	48.2	47.2	47.7	6.5	6.0	6.2	2
10	66.2	64.3	65.1	71.2	65.5	68.4	58.0	55.1	56.5	2.9	2.7	2.8	2
16	67.0	65.5	66.1	71.4	66.2	68.8	58.7	52.7	55.7	6.6	4.5	5.5	2
24	65.9	64.5	65.2	69.7	66.5	68.1	56.4	55.2	55.8	5.4	4.9	5.2	2
40	63.6	62.3	62.8	66.2	65.5	65.9	54.6	54.1	54.3	7.4	5.3	6.3	2
60	61.0	58.4	60.3	--	--	--	--	--	--	--	--	--	--
100	56.5	53.4	54.9	--	--	--	--	--	--	--	--	--	--

Table A6. *Strengthening response of 8090 as a function of aging at 350°F for a T5 temper. (The starting material was deformed to 0.6 SPF strain, Cold Water Quenched and naturally aged 1000 hours.)*

Aging Time (Hrs)	Hardness (HR30T)			Ult. Tens. Strength (ksi)			Yield Strength (ksi)			Elongation (%)			# of tests
	High	Low	Avg.	High	Low	Avg.	High	Low	Avg.	High	Low	Avg.	
1	55.9	53.9	54.5	58.0	56.2	57.1	44.2	43.5	44.0	5.9	4.2	5.1	3
3	58.5	55.6	57.0	64.4	61.3	62.5	50.5	45.5	47.5	6.8	5.0	6.1	3
10	60.9	59.2	60.0	66.2	63.5	65.0	51.5	49.4	50.7	5.3	4.2	4.7	3
16	63.7	61.1	62.2	68.4	64.1	65.9	53.9	49.0	50.7	8.9	4.4	6.6	3
24	65.4	62.0	63.9	67.5	60.2	62.0	54.8	49.1	51.1	3.6	1.3	2.7	6
40	66.8	64.2	65.3	72.6	68.6	70.0	59.7	54.4	56.0	6.8	4.3	5.7	6
60	67.2	65.2	66.0	73.7	71.9	72.8	59.8	57.4	58.6	7.2	5.6	6.3	3
100	67.2	65.2	65.7	72.5	69.8	71.1	61.1	55.9	58.3	6.9	5.5	6.3	3

Table A7. Strengthening response of 8090 as a function of aging at 375°F for a T5 temper. (The starting material was deformed to 0.6 SPF strain, Cold Water Quenched and naturally aged 1000 hours.)

Aging Time (Hrs)	Hardness (HR30T)			Ult. Tens. Strength (ksi)			Yield Strength (ksi)			Elongation (%)			# of tests
	High	Low	Avg.	High	Low	Avg.	High	Low	Avg.	High	Low	Avg.	
1	57.7	55.6	56.7	58.7	55.9	57.1	45.8	45.2	45.5	4.1	3.1	3.5	3
3	59.2	57.0	58.0	68.3	65.0	66.8	54.2	50.4	52.4	5.3	3.8	4.6	6
10	63.1	60.6	62.3	68.2	65.0	66.6	54.3	49.3	51.1	7.5	4.4	6.4	3
16	65.2	63.0	64.6	69.8	68.7	69.2	55.6	53.9	54.8	5.5	4.0	4.6	3
24	66.6	63.8	65.3	67.6	65.5	66.6	57.3	51.8	53.7	9.3	4.3	6.8	3
40	66.5	63.6	64.8	68.5	63.6	66.6	55.4	50.6	53.7	8.4	4.7	6.6	6
60	64.2	62.7	63.4	66.3	62.3	64.5	54.7	50.7	53.0	8.6	5.5	6.7	3
100	62.6	59.6	60.9	--	--	--	--	--	--	--	--	--	--

Table A8. Strengthening response of 8090 as a function of aging at 350°F for a T5 temper. (The starting material was deformed to 0.6 SPF strain, Accelerated Air Cooled and naturally aged 1000 hours.)

Aging Time (Hrs)	Hardness (HR30T)			Ult. Tens. Strength (ksi)			Yield Strength (ksi)			Elongation (%)			# of tests
	High	Low	Avg.	High	Low	Avg.	High	Low	Avg.	High	Low	Avg.	
1	59.4	57.8	58.6	62.0	59.7	60.7	46.8	44.8	45.7	6.6	5.9	6.3	3
3	61.4	59.0	60.1	--	--	--	--	--	--	--	--	--	--
10	63.8	62.8	63.3	67.0	63.5	65.1	51.9	49.9	50.7	5.6	3.9	4.7	3
16	65.3	63.9	64.8	--	--	--	--	--	--	--	--	--	--
24	65.7	64.8	65.2	68.3	66.4	67.6	53.9	51.6	53.0	6.2	4.2	5.1	3
40	67.0	65.9	66.5	69.9	67.8	69.1	54.9	54.0	54.5	7.5	5.3	6.3	3
60	68.4	66.7	67.5	71.4	68.6	69.8	57.3	55.4	56.2	6.1	4.8	5.5	3
100	67.7	66.2	66.7	69.7	62.7	66.4	56.5	52.4	54.4	7.2	5.7	6.4	3

Table A9. Strengthening response of 8090 as a function of aging at 375°F for a T5 temper. (The starting material was deformed to 0.6 SPF strain, Accelerated Air Cooled and naturally aged 1000 hours.)

Aging Time (Hrs)	Hardness (HR30T)			Ult. Tens. Strength (ksi)			Yield Strength (ksi)			Elongation (%)			# of tests
	High	Low	Avg.	High	Low	Avg.	High	Low	Avg.	High	Low	Avg.	
1	59.8	57.8	59.0	60.2	59.1	59.6	44.4	43.8	44.1	8.7	5.8	7.2	3
3	62.6	61.9	62.2	68.0	62.4	64.8	50.2	47.0	48.8	6.9	4.6	5.9	6
10	66.1	64.7	65.3	68.3	65.3	66.9	53.7	51.5	52.0	6.9	4.2	5.5	6
16	67.8	65.1	66.0	67.3	67.0	67.1	53.3	52.0	52.6	8.6	5.1	6.5	3
24	67.2	66.5	66.8	68.8	67.4	68.3	55.4	53.3	54.6	8.7	5.5	7.3	3
40	65.7	64.5	65.2	65.0	64.8	64.9	52.2	51.5	51.8	7.3	6.1	6.5	3
60	64.2	62.9	63.7	--	--	--	--	--	--	--	--	--	--
100	57.0	56.6	56.8	--	--	--	--	--	--	--	--	--	--

Table A10. Age hardening behavior of 2090 as a function of temperature and SPF strain (ϵ) for material Cold Water Quenched following forming for a T5 temper. Units: Rockwell Superficial Hardness (30T scale).

Temp. (°F)	Time (Hrs)	ϵ = 0			ϵ = 0.3			ϵ = 0.6		
		High	Low	Avg.	High	Low	Avg.	High	Low	Avg.
325	1	55.5	53.7	54.7	56.7	55.1	55.8	50.5	49.5	50.1
	3	61.2	59.6	60.5	60.6	59.6	60.0	55.5	54.6	55.1
	10	63.4	62.4	62.7	62.7	61.5	61.8	59.1	56.0	57.8
	16	64.6	63.7	64.0	64.2	63.3	63.8	60.0	58.3	59.3
	24	65.6	64.1	64.9	65.7	64.8	65.1	61.6	61.1	61.4
	36	66.2	65.4	65.8	67.4	65.9	67.0	64.8	60.9	62.8
	72	66.1	65.8	65.9	68.5	66.4	67.7	66.5	62.3	65.1
	100	66.4	65.5	66.1	69.3	67.1	68.0	66.0	64.6	65.1
350	1	59.4	58.9	59.2	60.5	59.4	60.0	54.7	53.6	54.0
	3	63.9	62.1	62.8	62.7	61.8	62.2	57.7	56.7	57.3
	10	64.8	63.7	64.3	66.0	64.7	65.1	61.6	60.7	61.2
	16	65.4	63.9	64.6	65.7	65.3	65.5	64.3	60.9	62.3
	24	67.1	64.4	66.1	66.8	65.9	66.5	64.5	63.6	64.2
	36	66.4	65.4	65.9	67.2	66.4	66.8	69.0	67.8	68.2
	72	66.5	65.0	65.9	67.9	67.1	67.5	65.9	65.3	65.6
	100	66.5	64.3	65.6	67.3	66.8	67.1	65.8	64.5	64.9
375	1	59.3	58.7	59.0	59.7	56.7	58.4	56.5	51.8	54.5
	3	62.4	58.1	59.8	61.6	60.7	61.2	58.7	57.1	57.8
	10	64.2	62.5	63.3	65.4	63.7	64.6	63.0	61.8	62.4
	16	66.2	65.5	65.7	65.7	64.9	65.3	64.0	62.0	63.0
	24	64.9	64.1	64.6	67.4	66.5	67.1	69.5	66.5	67.8
	36	64.7	63.4	64.2	66.2	64.8	65.4	66.0	64.6	65.3
	72	63.9	62.8	63.6	65.3	64.7	65.1	64.6	64.3	64.4
	100	62.6	61.8	62.3	64.3	62.5	63.5	64.2	63.1	63.6

Table A11. Age hardening behavior of 2090 as a function of temperature and SPF strain (ϵ) for material Accelerated Air Cooled following forming for a T5 temper. Units: Rockwell Superficial Hardness (30T scale).

Temp. (°F)	Time (Hrs)	ϵ = 0			ϵ = 0.3			ϵ = 0.6		
		High	Low	Avg.	High	Low	Avg.	High	Low	Avg.
325	1	57.2	56.3	56.9	58.2	57.3	57.7	49.5	48.9	49.1
	3	61.6	59.3	60.3	60.0	59.5	59.7	56.9	55.6	56.3
	10	62.6	61.8	62.3	62.7	62.5	62.6	57.8	56.1	57.1
	16	64.2	63.2	63.7	63.9	63.1	63.4	59.5	58.8	59.1
	24	64.7	63.7	64.2	65.6	65.1	65.4	63.1	58.8	61.0
	36	64.6	64.1	64.3	66.3	65.5	65.9	63.0	61.7	62.5
	72	64.9	64.6	64.7	66.9	65.6	66.2	64.2	62.0	63.0
	100	65.8	65.0	65.4	67.7	65.9	66.7	64.2	63.2	63.8
350	1	58.1	57.5	57.7	60.1	59.2	59.8	52.9	50.7	52.0
	3	60.6	60.1	60.4	63.2	61.5	62.4	57.4	56.0	56.6
	10	62.5	61.9	62.2	63.4	62.7	63.0	60.5	59.1	60.0
	16	63.9	63.1	63.4	64.1	63.6	63.9	61.2	60.1	60.4
	24	63.7	62.9	63.4	65.3	63.7	64.3	62.0	60.4	61.3
	36	63.0	62.1	62.6	65.3	65.1	65.2	62.0	61.0	61.5
	72	64.1	61.1	62.5	65.2	63.7	64.6	61.9	59.4	60.4
	100	63.0	61.9	62.4	64.6	64.3	64.5	58.6	57.2	57.9
375	1	58.7	58.2	58.5	61.0	60.4	60.7	57.2	55.5	56.4
	3	62.3	61.4	61.7	62.6	61.1	61.6	58.3	55.4	57.2
	10	63.2	62.6	62.8	63.7	62.8	63.3	62.1	59.2	60.9
	16	63.0	61.5	62.3	64.4	63.6	64.0	62.3	60.0	61.5
	24	62.5	61.9	62.1	64.8	63.5	64.1	63.8	61.3	62.6
	36	61.8	60.7	61.2	63.9	63.5	63.7	60.6	59.3	59.8
	72	58.6	58.1	58.3	63.0	62.1	62.5	58.9	57.4	58.1
	100	58.0	57.2	57.6	60.8	60.1	60.5	55.5	52.5	54.5

Table A12. Strengthening response of 2090 as a function of aging at 350°F for a T6 temper. (The starting material was deformed to 0.6 SPF strain, air cooled, Solution Heat Treated, cold water quenched and naturally aged 100 hours.)

Aging Time (Hrs)	Hardness (HR30T)			Ult. Tens. Strength (ksi)			Yield Strength (ksi)			Elongation (%)			# of tests
	High	Low	Avg.	High	Low	Avg.	High	Low	Avg.	High	Low	Avg.	
1	58.0	52.1	55.2	61.6	61.2	61.4	48.3	48.2	48.3	8.5	7.2	7.8	2
3	60.8	58.6	60.1	64.6	62.5	63.7	51.2	50.0	50.7	6.6	5.8	6.2	3
10	64.6	63.9	64.3	67.5	66.1	66.8	56.9	56.7	56.8	3.7	2.9	3.3	2
16	65.9	64.9	65.3	70.2	68.4	69.3	58.0	56.7	57.4	4.3	4.2	4.2	2
24	69.2	62.5	66.5	71.2	70.4	70.8	62.1	59.1	60.6	3.9	2.9	3.4	2
40	68.8	66.8	67.6	72.5	71.8	72.1	63.3	61.1	62.2	5.4	4.8	5.1	2
60	69.8*	65.8*	67.7*	72.4	72.1	72.3	66.2	64.7	65.5	4.1	1.7	2.9	2
100	70.5	63.6	67.1	--	--	--	--	--	--	--	--	--	--

* *70 hour hardness data*

Table A13. Strengthening response of 2090 as a function of aging at 325°F for a T5 temper. (The starting material was deformed to 0.6 SPF strain, Cold Water Quenched and naturally aged 1000 hours.)

Aging Time (Hrs)	Hardness (HR30T)			Ult. Tens. Strength (ksi)			Yield Strength (ksi)			Elongation (%)			# of tests
	High	Low	Avg.	High	Low	Avg.	High	Low	Avg.	High	Low	Avg.	
1	50.5	49.5	50.1	57.6	55.1	56.2	49.8	42.4	45.0	6.7	5.6	6.1	3
3	55.5	54.6	55.1	--	--	--	--	--	--	--	--	--	--
10	59.1	56.0	57.8	65.2	63.2	64.6	53.1	51.7	52.3	6.4	4.6	5.7	3
16	60.0	58.3	59.3	--	--	--	--	--	--	--	--	--	--
24	61.6	61.1	61.4	67.3	66.4	66.7	55.1	53.7	54.5	6.7	4.9	5.8	3
40	64.8*	60.9*	62.8*	69.3	66.6	68.3	55.7	55.1	55.3	7.3	3.7	5.5	3
60	66.5**	62.3**	65.1**	70.5	68.8	69.8	57.8	56.2	56.7	6.5	4.2	5.1	3
100	66.0	64.6	65.1	71.7	69.2	70.4	58.8	56.5	57.4	6.2	5.0	5.8	3

** 36 hour / ** 72 hour hardness data*

Table A14. Strengthening response of 2090 as a function of aging at 350°F for a T5 temper. (The starting material was deformed to 0.6 SPF strain, Cold Water Quenched and naturally aged 1000 hours.)

Aging Time (Hrs)	Hardness (HR30T)			Ult. Tens. Strength (ksi)			Yield Strength (ksi)			Elongation (%)			# of tests
	High	Low	Avg.	High	Low	Avg.	High	Low	Avg.	High	Low	Avg.	
1	54.7	53.6	54.0	61.2	56.3	58.3	47.7	46.4	46.9	9.0	4.1	6.2	3
3	57.7	56.7	57.3	63.7	63.2	63.4	50.9	50.2	50.5	6.6	5.4	6.2	3
10	61.6	60.7	61.2	68.7	65.8	67.1	55.5	52.8	53.8	6.8	4.9	5.8	5
16	64.3	60.9	62.3	67.4	65.1	66.3	54.9	52.2	53.2	6.5	4.7	5.5	3
24	64.5	63.6	64.2	70.6	67.9	69.1	59.4	54.7	56.3	6.8	5.3	6.1	3
40	68.2*	66.9*	67.7*	69.3	66.9	67.8	56.8	54.2	55.5	6.0	4.9	5.5	3
60	65.9**	65.3**	65.6**	69.3	67.1	68.1	57.8	55.5	56.8	5.7	4.4	4.9	3
100	65.8	64.5	64.9	--	--	--	--	--	--	--	--	--	--

** 36 hour / ** 72 hour hardness data*

Table A15. Strengthening response of 2090 as a function of aging at 325°F for a T5 temper. (The starting material was deformed to 0.6 SPF strain, Accelerated Air Cooled and naturally aged 1000 hours.)

Aging Time (Hrs)	Hardness (HR30T)			Ult. Tens. Strength (ksi)			Yield Strength (ksi)			Elongation (%)			# of tests
	High	Low	Avg.	High	Low	Avg.	High	Low	Avg.	High	Low	Avg.	
1	49.5	48.9	49.1	60.5	58.6	59.6	45.4	44.3	44.9	8.1	7.8	8.0	3
3	56.9	55.6	56.3	--	--	--	--	--	--	--	--	--	--
10	57.8	56.1	57.1	65.4	63.2	64.3	52.6	50.7	51.7	6.0	4.9	5.4	2
16	59.5	58.8	59.1	--	--	--	--	--	--	--	--	--	--
24	63.1	58.8	61.0	70.8	67.8	69.0	57.2	55.3	56.0	5.9	5.0	5.4	3
40	63.0*	61.7*	62.5*	72.6	69.3	70.8	59.4	57.3	58.3	5.7	5.4	5.5	2
60	64.2**	62.0**	63.0**	71.1	69.7	70.3	57.5	56.7	57.0	5.9	4.1	5.1	3
100	64.2	63.2	63.8	71.8	70.1	70.9	60.0	59.1	59.4	6.1	3.6	4.8	3

** 36 hour / ** 72 hour hardness data*

Table A16. Strengthening response of 2090 as a function of aging at 350°F for a T5 temper. (The starting material was deformed to 0.6 SPF strain, Accelerated Air Cooled and naturally aged 1000 hours.)

Aging Time (Hrs)	Hardness (HR30T)			Ult. Tens. Strength (ksi)			Yield Strength (ksi)			Elongation (%)			# of tests
	High	Low	Avg.	High	Low	Avg.	High	Low	Avg.	High	Low	Avg.	
1	52.9	50.7	52.0	63.2	61.0	62.3	49.3	47.9	48.5	9.0	8.0	8.5	3
3	57.4	56.0	56.6	--	--	--	--	--	--	--	--	--	--
10	60.5	59.1	60.0	68.9	67.6	68.1	55.8	54.4	54.9	6.8	5.2	5.8	3
16	61.2	60.1	60.4	69.5	68.3	68.9	55.5	55.3	55.4	6.2	6.0	6.1	2
24	62.0	60.4	61.3	70.1	69.5	69.8	57.9	56.1	57.1	7.0	5.1	6.0	3
40	62.0*	61.0*	61.5*	68.0	67.3	67.8	56.0	54.9	55.3	7.6	4.7	6.2	3
60	61.9**	59.4**	60.4**	67.4	66.7	67.0	55.8	54.3	54.9	7.4	5.4	6.3	3
100	58.6	57.2	57.9	--	--	--	--	--	--	--	--	--	--

** 36 hour / ** 72 hour hardness data*

Table A17. Age hardening behavior of X2095 as a function of temperature and SPF strain (ϵ) for material Cold Water Quenched following forming for a T5 temper. Units: Rockwell Superficial Hardness (45T scale).

Temp. (°F)	Time (Hrs)	ϵ = 0			ϵ = 0.3			ϵ = 0.6		
		High	Low	Avg.	High	Low	Avg.	High	Low	Avg.
325	1	37.3	35.7	36.2	32.3	30.8	31.8	29.3	26.9	28.0
	3	41.5	40.5	41.0	38.2	36.9	37.4	36.1	34.3	35.2
	10	49.8	48.3	49.2	53.3	51.8	52.4	46.8	45.1	46.1
	16	55.5	54.2	54.9	59.9	57.5	58.5	53.3	51.9	52.6
	24	59.7	59.0	59.4	61.4	60.7	61.1	58.9	57.2	58.0
	40	65.7	64.6	65.0	65.9	65.0	65.5	65.2	64.0	64.8
	60	67.5	67.3	67.3	67.9	66.9	67.5	67.0	66.4	66.7
	100	67.9	67.6	67.8	69.1	67.7	68.6	69.2	67.2	68.2
350	1	46.9	45.9	46.3	47.1	46.0	46.4	41.0	39.7	40.3
	3	55.1	53.3	54.2	56.7	55.3	56.1	52.5	51.5	51.8
	10	65.9	65.3	65.6	67.0	66.3	66.6	65.8	64.8	65.2
	16	68.9	67.4	68.2	68.4	66.6	67.4	66.9	65.9	66.5
	24	68.8	68.1	68.5	70.3	68.5	69.3	68.4	66.9	67.6
	40	69.1	68.3	68.8	70.4	69.3	69.9	69.1	67.9	68.4
	60	68.8	67.8	68.3	70.6	69.0	69.7	68.8	66.9	67.7
	100	68.3	67.3	67.9	68.6	67.8	68.1	67.0	64.7	65.7
375	1	52.9	51.8	52.2	54.0	53.1	53.5	51.0	49.5	50.5
	3	63.8	61.6	62.5	65.2	64.3	64.6	64.6	62.3	63.5
	10	66.3	65.4	65.9	68.0	64.6	66.8	66.9	65.3	66.0
	16	67.3	66.1	66.7	67.6	66.7	67.1	67.1	66.5	66.8
	24	66.4	65.4	66.0	67.2	65.7	66.4	65.6	65.1	65.4
	40	65.9	65.2	65.6	66.2	64.8	65.5	65.6	63.1	64.5
	60	63.5	62.3	63.0	64.4	62.9	63.9	63.1	61.5	62.5
	100	61.1	60.1	60.8	62.6	61.3	62.0	59.5	58.1	58.5

Table A18. Age hardening behavior of X2095 as a function of temperature and SPF strain (ϵ) for material Accelerated Air Cooled following forming for a T5 temper. Units: Rockwell Superficial Hardness (45T scale).

Temp. (°F)	Time (Hrs)	ϵ = 0			ϵ = 0.3			ϵ = 0.6		
		High	Low	Avg.	High	Low	Avg.	High	Low	Avg.
325	1	31.3	28.7	30.0	30.4	29.4	30.0	24.1	21.4	23.1
	3	32.4	29.6	30.9	30.4	28.8	29.4	24.5	20.7	22.6
	10	36.4	35.4	36.0	38.5	36.9	37.8	38.0	36.8	37.4
	16	41.0	40.2	40.5	40.7	40.1	40.5	40.5	39.8	40.1
	24	49.7	48.3	48.9	50.9	50.5	50.7	51.0	50.2	50.5
	40	51.4	50.5	50.8	55.3	54.6	54.9	54.7	53.8	54.2
	60	54.5	54.1	54.3	56.0	54.5	55.3	56.7	56.4	56.5
	100	56.0	54.4	55.3	59.6	57.9	58.9	60.0	59.3	59.5
350	1	36.8	33.1	35.5	37.6	36.7	37.2	36.2	35.1	35.8
	3	42.9	42.0	42.5	44.8	43.6	44.2	44.8	43.5	44.1
	10	48.0	47.3	47.8	52.3	51.1	51.7	53.1	51.9	52.5
	16	53.5	52.4	53.1	57.2	56.7	57.0	57.6	56.5	56.9
	24	56.8	55.3	55.8	59.5	58.4	58.8	58.7	56.9	57.7
	40	56.9	55.1	56.1	57.6	56.4	57.1	58.4	57.3	58.1
	60	51.7	50.4	51.1	58.1	57.1	57.7	58.1	55.6	56.9
	100	48.7	47.8	48.4	56.4	55.8	56.0	55.8	51.7	54.0
375	1	40.8	39.0	39.9	41.2	40.0	40.6	40.2	39.0	39.4
	3	39.8	38.5	39.4	47.8	46.2	47.1	49.3	48.1	48.6
	10	51.5	50.3	50.6	54.1	53.0	53.5	53.6	52.9	53.3
	16	55.4	50.8	53.2	53.9	52.8	53.2	55.2	54.7	54.9
	24	53.6	49.0	52.2	53.7	52.6	53.2	53.6	53.1	53.4
	40	50.3	46.1	48.3	56.7	54.9	55.7	56.3	55.6	56.0
	60	50.3	47.2	49.6	52.1	50.8	51.5	51.7	50.8	51.3
	100	45.2	42.7	44.2	50.6	50.4	50.5	48.4	46.1	47.3

Table A19. Strengthening response of X2095 as a function of aging at 350°F for a T6 temper. (The starting material was deformed to 0.6 SPF strain, air cooled, Solution Heat Treated, cold water quenched and naturally aged 100 hours.)

Aging Time (Hrs)	Hardness (HR45T)			Ult. Tens. Strength (ksi)			Yield Strength (ksi)			Elongation (%)			# of tests
	High	Low	Avg.	High	Low	Avg.	High	Low	Avg.	High	Low	Avg.	
1	38.2	35.3	36.7	76.2	75.6	75.9	53.6	52.4	53.0	18.4	14.1	16.3	2
3	52.7	43.5	47.9	77.5	76.5	77.0	61.1	59.4	60.0	16.5	13.0	15.0	3
10	61.9	59.6	61.1	93.5	90.1	92.0	87.9	85.8	86.9	5.5	2.3	4.0	3
16	65.2	63.2	64.3	94.5	94.4	94.4	90.7	90.1	90.4	4.7	2.8	3.8	2
24	66.9	64.3	65.7	95.0	93.3	94.1	91.2	89.5	90.4	3.3	2.6	2.9	2
40	67.1	65.0	66.4	94.5	94.0	94.3	91.5	91.2	91.4	2.6	2.2	2.4	2
60	65.9	64.4	65.3	92.6	92.3	92.5	88.9	87.8	88.3	3.9	2.4	3.1	2
100	63.7	62.0	62.6	--	--	--	--	--	--	--	--	--	--

Table A20. Strengthening response of X2095 as a function of aging at 325°F for a T5 temper. (The starting material was deformed to 0.6 SPF strain, Cold Water Quenched and naturally aged 1000 hours.)

Aging Time (Hrs)	Hardness (HR45T)			Ult. Tens. Strength (ksi)			Yield Strength (ksi)			Elongation (%)			# of tests
	High	Low	Avg.	High	Low	Avg.	High	Low	Avg.	High	Low	Avg.	
1	29.3	26.9	28.0	68.5	66.1	67.0	43.3	41.6	42.2	19.9	19.2	19.6	3
3	36.1	34.3	35.2	71.6	68.9	70.2	43.0	42.2	42.5	23.8	21.8	23.0	3
10	46.8	45.1	46.1	78.4	77.6	78.1	58.8	57.9	58.4	16.9	13.6	15.5	3
16	53.3	51.9	52.6	83.4	81.6	82.2	71.6	68.6	70.0	13.3	10.6	11.7	3
24	58.9	57.2	58.0	83.0	82.0	82.6	74.2	73.0	73.7	7.2	6.7	6.9	3
40	65.2	64.0	64.8	92.3	91.8	92.1	87.7	87.1	87.5	4.6	3.0	3.8	3
60	67.0	66.4	66.7	93.3	92.8	93.1	89.7	88.4	88.9	3.1	2.4	2.7	3
100	69.2	67.2	68.2	93.2	93.0	93.1	89.7	89.2	89.6	2.3	1.2	1.9	3

Table A21. Strengthening response of X2095 as a function of aging at 350°F for a T5 temper. (The starting material was deformed to 0.6 SPF strain, Cold Water Quenched and naturally aged 1000 hours.)

Aging Time	Hardness (HR45T)			Ult. Tens. Strength (ksi)			Yield Strength (ksi)			Elongation (%)			# of tests
	High	Low	Avg.	High	Low	Avg.	High	Low	Avg.	High	Low	Avg.	
1	41.0	39.7	40.3	71.8	71.3	71.6	49.2	48.9	49.0	20.8	19.0	19.8	3
3	52.5	51.5	51.8	79.3	77.5	78.5	63.5	60.4	62.0	14.8	13.1	14.0	3
10	65.8	64.8	65.2	92.4	88.1	90.8	87.6	83.0	85.7	4.6	3.5	4.2	3
16	66.9	65.9	66.5	94.2	92.4	93.5	89.2	88.4	88.9	3.3	2.1	2.9	3
24	68.4	66.9	67.6	98.8	94.7	96.9	97.0	91.7	94.8	2.8	2.2	2.5	3
40	69.1	67.9	68.4	95.4	95.0	95.2	90.4	89.2	89.7	2.4	1.3	1.7	3
60	68.8	66.9	67.7	96.2	91.1	94.1	90.8	86.3	88.7	1.9	1.8	1.8	3
100	67.0	64.7	65.7	--	--	--	--	--	--	--	--	--	--

Table A22. Strengthening response of X2095 as a function of aging at 325°F for a T5 temper. (The starting material was deformed to 0.6 SPF strain, Accelerated Air Cooled and naturally aged 1000 hours.)

Aging Time (Hrs)	Hardness (HR45T)			Ult. Tens. Strength (ksi)			Yield Strength (ksi)			Elongation (%)			# of tests
	High	Low	Avg.	High	Low	Avg.	High	Low	Avg.	High	Low	Avg.	
1	24.1	21.4	23.1	69.8	69.0	69.3	44.3	42.8	43.4	19.6	17.0	17.9	3
3	24.5	20.7	22.6	65.8	65.3	65.6	38.6	37.8	38.1	21.4	17.6	19.4	3
10	38.0	36.8	37.4	72.3	70.3	71.2	48.3	46.6	47.5	15.8	12.8	14.2	3
16	40.5	39.8	40.1	74.0	72.2	73.0	57.6	54.0	56.1	14.1	12.3	13.2	3
24	51.0	50.2	50.5	78.9	78.1	78.5	66.1	65.0	65.6	8.2	7.2	7.7	2
40	54.7	53.8	54.2	81.6	81.2	81.3	71.4	70.5	70.9	5.4	4.8	5.1	3
60	56.7	56.4	56.5	84.6	83.0	84.0	75.0	73.3	74.3	4.7	2.9	3.9	3
100	60.0	59.3	59.5	84.1	84.0	84.1	74.7	74.6	74.7	3.1	3.0	3.1	2

Table A23. Strengthening response of X2095 as a function of aging at 350°F for a T5 temper. (The starting material was deformed to 0.6 SPF strain, Accelerated Air Cooled and naturally aged 1000 hours.)

Aging Time (Hrs)	Hardness (HR45T)			Ult. Tens. Strength (ksi)			Yield Strength (ksi)			Elongation (%)			# of tests
	High	Low	Avg.	High	Low	Avg.	High	Low	Avg.	High	Low	Avg.	
1	36.2	35.1	35.8	72.2	70.4	71.6	47.5	46.3	47.1	17.7	17.4	17.5	3
3	44.8	43.5	44.1	71.4	70.6	71.2	49.4	48.8	49.0	17.9	13.8	16.2	3
10	53.1	51.9	52.5	81.7	78.5	80.4	67.5	65.2	66.5	6.3	5.4	6.0	3
16	57.6	56.5	56.9	82.8	82.5	82.7	71.7	69.9	70.7	4.8	4.7	4.7	3
24	58.7	56.9	57.7	83.0	81.4	82.4	72.2	70.5	71.1	5.0	3.3	4.1	3
40	58.4	57.3	58.1	83.1	81.8	82.4	71.8	70.3	71.3	4.0	2.5	3.4	3
60	58.1	55.6	56.9	83.3	81.8	82.7	72.8	70.0	71.3	3.2	1.6	2.6	3
100	55.8	51.7	54.0	--	--	--	--	--	--	--	--	--	--

REPORT DOCUMENTATION PAGE

Form Approved
OMB No. 0704-0188

1. AGENCY USE ONLY (Leave blank)	2. REPORT DATE	3. REPORT TYPE AND DATES COVERED
	September 1993	Contractor Report

4. TITLE AND SUBTITLE

Effect of Thermal Processing Practices on the Properties of Superplastic Al-Li Alloys

5. FUNDING NUMBERS

C NAS1-19399

WU 505-63-50-03

6. AUTHOR(S)

Stephen J. Hales and Henry E. Lippard

7. PERFORMING ORGANIZATION NAME(S) AND ADDRESS(ES)

Analytical Services & Materials, Inc.
107 Research Drive
Hampton, VA 23666

8. PERFORMING ORGANIZATION REPORT NUMBER

9. SPONSORING/MONITORING AGENCY NAME(S) AND ADDRESS(ES)

NASA Langley Research Center
Hampton, VA 23681-0001

10. SPONSORING/MONITORING AGENCY REPORT NUMBER

NASA CR-4548

11. SUPPLEMENTARY NOTES

Stephen J. Hales: Analytical Services & Materials, Inc., Hampton, VA
Henry E. Lippard: Northwestern University, Dept. of Materials Science, Evanston, IL
Langley Technical Monitor: Thomas T. Bales Final Report

12a. DISTRIBUTION/AVAILABILITY STATEMENT

Unclassified - Unlimited

Subject Category 26

12b. DISTRIBUTION CODE

13. ABSTRACT *(Maximum 200 words)*

The effect of thermal processing on the mechanical properties of superplastically formed structural components fabricated from three aluminum-lithium alloys was evaluated. The starting materials consisted of 8090, 2090 and X2095 (Weldalite™049), in the form of commercial-grade superplastic sheet. The experimental test matrix was designed to assess the impact on mechanical properties of eliminating solution heat treatment and/or cold water quenching from post-forming thermal processing. The extensive hardness and tensile property data compiled are presented as a function of aging temperatire, superplastic strain and temper/quench rate for each alloy. The tensile properties of the materials following superplastic forming in two T5-type tempers are compared with the baseline T6 temper. The implications for simplifying thermal processing without degradation in properties are discussed on the basis of the results.

14. SUBJECT TERMS		15. NUMBER OF PAGES
Aluminum-Lithium Alloys Superplastic Forming Heat Treatment	Mechanical properties	68
		16. PRICE CODE A04

17. SECURITY CLASSIFICATION OF REPORT	18. SECURITY CLASSIFICATION OF THIS PAGE	19. SECURITY CLASSIFICATION OF ABSTRACT	20. LIMITATION OF ABSTRACT
UNCLASSIFIED	UNCLASSIFIED	UNCLASSIFIED	

NSN 7540-01-280-5500

Standard Form 298 (Rev. 2-89)
Prescribed by ANSI Std. Z39-18
298-102

☆U.S. GOVERNMENT PRINTING OFFICE: 1993 - 728-064/86059